

Non-Hermitian phase transition from a polariton Bose-Einstein condensate to a photon laser

Ryo Hanai,^{1,2,*} Alexander Edelman,¹ Yoji Ohashi,³ and Peter B. Littlewood^{1,4}

¹*James Franck Institute and Department of Physics, University of Chicago, Illinois, 60637, USA*

²*Department of Physics, Osaka University, Toyonaka 560-0043, Japan*

³*Department of Physics, Keio University, Yokohama 223-8522, Japan*

⁴*Materials Science Division, Argonne National Laboratory, Argonne, Illinois 60439, USA*

(Dated: December 15, 2024)

We propose a novel mechanism for a nonequilibrium phase transition within a $U(1)$ -broken phase of an electron-hole-photon system, from a Bose-Einstein condensate of polaritons to a photon laser, induced by the non-Hermitian nature of the condensate. We show that a (uniform) steady state of the condensate can always be classified into two types, namely, arising either from lower or upper-branch polaritons. We prove (for a general model) and demonstrate (for a particular model of polaritons) that an exceptional point where the two types coalesce marks the endpoint of a first-order-like phase boundary between the two types, similar to a critical point in a liquid-gas phase transition. Since the phase transition found in this paper is not in general triggered by population inversion, our result implies that the second threshold observed in experiments is not necessarily a strong-to-weak-coupling transition, contrary to the widely-believed understanding. Although our calculation mainly aims to clarify polariton physics, our discussion applies to general driven-dissipative condensates composed of two complex fields.

PACS numbers:

The phenomenon of macroscopic condensation has been one of the principal topics in modern condensed matter physics and optics [1]. The central example is, of course, Bose-Einstein condensation (BEC), which has been observed in various systems, ranging from atomic gases [2, 3], liquid ^4He [4], exciton-polaritons [5–8], magnons [9–11], photons [12], to plasmonic lattice polaritons [13]. In these systems, thermalization plays a crucial role in achieving macroscopic occupation of the lowest energy level. A photon laser [14, 15], in contrast, is a nonequilibrium condensate, where the population inversion in an optical gain medium induces macroscopic coherence.

The semiconductor microcavity system [5–8] provides a unique opportunity to study similarities and differences of these two classes of condensation phenomena [16], since it can exhibit both [17], by tuning the pump power. At low pump power where hybrid light-matter quasiparticles called polaritons form (so-called strong coupling), thermalization is efficient due to relaxation processes such as stimulated scattering of polaritons. This makes it possible for the system to turn into a polariton-BEC, once the pump power exceeds a certain threshold [5]. At high power, in contrast, the system operates as a vertical-cavity surface-emitting laser (VCSEL), which is a type of a photon laser, with electrons and holes acting as a gain medium. Interestingly, a number of experiments [18–28] suggest that there exists a phase boundary between the two regions, where a second threshold has been observed, traditionally interpreted as a transition to a (weak coupling) VCSEL.

This two-threshold-behavior presents a theoretical challenge, however. The phase transition to photon las-

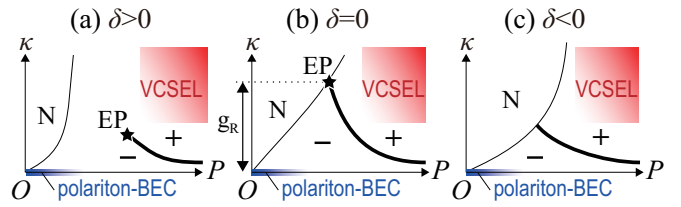


FIG. 1: (Color online) Proposed phase diagram of a driven-dissipative electron-hole-photon gas, in terms the photon decay rate κ and the pump power P . (a) Blue detuning. (b) On resonance. (c) Red detuning. “ $-(+)$ ” represents the “ $-(+)$ ”-solution phase, “N” represents the normal phase, “EP” is the exceptional point, and g_R is the Rabi splitting. The thick (thin) solid line represents the phase boundary in the condensed phase (between the normal and the condensed phase).

ing is associated with breaking a $U(1)$ symmetry, but the polariton-BEC, which arises after the first threshold, is already in a $U(1)$ -broken phase. Thus, there seems to be no good reason to expect a second phase transition. Indeed, to our knowledge, all theories to date predict a crossover [29–33].

In this paper, we propose a novel mechanism for a phase transition within the $U(1)$ -broken phase, triggered by the non-Hermitian nature of the out-of-equilibrium condensate. Using an exact equations of motion approach, we clarify that the steady states of a two-component condensate of electron-hole pairs and photons can be classified into two types of solutions, corresponding to condensation to different branches of the polariton spectra. We find that an exceptional point (EP), where the two solutions coalesce [34–41], may appear due to the

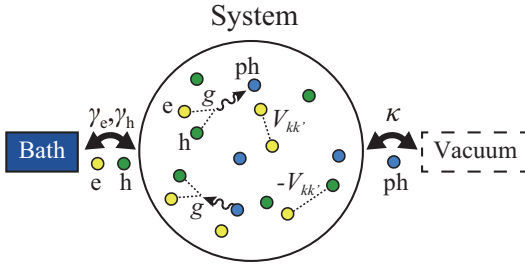


FIG. 2: (Color online) Model driven-dissipative electron-hole-photon gas. The system is attached to an electron-hole bath and a photon vacuum. Electrons (holes) are incoherently supplied to the system with the rate $\gamma_{e(h)}$. In the system, the injected electrons (“e”) and holes (“h”) repulsively (e-e, h-h) and attractively (e-h) interact with the Coulomb potential $V_{\mathbf{k}-\mathbf{k}'} = e^2/(2\epsilon|\mathbf{k} - \mathbf{k}'|)$. The electrons and holes pair-annihilate (create) to create (annihilate) cavity-photons (“ph”) via the dipole coupling g between the electron-hole carriers and the cavity-photons. The created photons in the cavity leak out to the vacuum with the decay rate κ .

non-Hermiticity of the equation of motion. We prove and demonstrate that this is the endpoint of a first-order-like phase transition line between the two solutions. Based on these results, we propose a phase diagram of an electron-hole-photon system depicted in Fig. 1; we show the phase boundary between the polariton-BEC and VCSEL in the red detuning case $\delta < 0$ [panel (c)], as well as the boundary being accompanied by an endpoint in the blue detuning case $\delta > 0$ [panel (a)].

The phase transition found in this paper is ultimately caused by the non-orthogonality of the eigenmodes of the coupled electron-hole with photon coherent fields. Thus, our discussion is applicable to any driven-dissipative condensate composed of two complex fields with balanced gain and loss [42–44]. Because the transition is insensitive to details of the system such as the presence of population inversion, our finding implies that it may happen in the strong-coupling regime as well, contrary to the ordinary understanding.

We use a microscopic model schematically shown in Fig. 2 [31–33, 45], which has been shown to capture both the essential physics of the BEC state and the VCSEL [31–33], as well as to give a semiquantitative agreement [45] with photoluminescence experiments [21, 46–48]. The system is composed of electrons, holes, and cavity-photons, and they are coupled to an electron-hole bath and a photon vacuum. Electrons (holes) are incoherently pumped to the system from the bath at a rate $\gamma_{e(h)}$. The injected electrons and holes Coulomb-interact with each other and create (annihilate) photons by pair-annihilation (creation). The photons leak out to the vacuum with the decay rate κ , driving the system into a non-equilibrium steady state. The explicit expression for the Hamiltonian H is given in the Supplemental Material

[49].

We apply the Keldysh Green’s function method [50] to the model. As shown in Ref. [49] in a formally exact way, the dynamics of the electron-hole dipole polarization $p_{\mathbf{k}}(\mathbf{r}, t)$ and the electron (hole) density $n_{\mathbf{k}, \sigma=e(h)}(\mathbf{r}, t)$ obeys the generalized Boltzmann equation,

$$i\hbar\partial_t p_{\mathbf{k}}(\mathbf{r}, t) = \left[\varepsilon_{\mathbf{k}, e} + \varepsilon_{\mathbf{k}, h} - \frac{\hbar^2 \nabla^2}{4m_{e(h)}} - 2i\gamma \right] p_{\mathbf{k}}(\mathbf{r}, t) - \sum_{\mathbf{k}'} L_{\mathbf{k}, \mathbf{k}'}(\mathbf{r}, t) \Delta_{\mathbf{k}'}(\mathbf{r}, t), \quad (1)$$

$$\partial_t n_{\mathbf{k}, \sigma}(\mathbf{r}, t) + \mathbf{v}_{\mathbf{k}, \sigma} \cdot \nabla n_{\mathbf{k}, \sigma}(\mathbf{r}, t) = -\frac{2\gamma_{\sigma}}{\hbar} n_{\mathbf{k}, \sigma}(\mathbf{r}, t) + I_{\mathbf{k}, \sigma}(\mathbf{r}, t). \quad (2)$$

Here, $\varepsilon_{\mathbf{k}, e(h)} = \hbar^2 \mathbf{k}^2 / (2m_{e(h)}) + E_g/2$ is the dispersion of the electron (hole) in the conduction (valence) band, where $m_{e(h)}$ is the effective mass of electrons (holes). E_g is the energy gap of the semiconductor material. $m_{eh} = 2m_e m_h / (m_e + m_h)$ is twice the reduced mass of an electron and a hole, and $\mathbf{v}_{\mathbf{k}, e(h)} = \hbar \mathbf{k} / m_{e(h)}$. We have introduced the order parameter $\Delta_{\mathbf{k}}(\mathbf{r}, t) = \sum_{\mathbf{k}'} V_{\mathbf{k}-\mathbf{k}'} p_{\mathbf{k}'}(\mathbf{r}, t) - g \lambda_{\text{cav}}(\mathbf{r}, t)$ describing the condensed phase, where $\lambda_{\text{cav}}(\mathbf{r}, t) = \langle a(\mathbf{r}, t) \rangle$ is the coherent cavity-photon amplitude (where $a(\mathbf{r}, t)$ is the annihilation operator of a cavity-photon), $V_{\mathbf{k}} = e^2 / (2\epsilon|\mathbf{k}|)$ is the two-dimensional Coulomb interaction (ϵ is the dielectric constant), and g is a dipole coupling between carriers (electrons and holes) and photons. The coupling of the system to the bath causes the dephasing/decay of $p_{\mathbf{k}}(\mathbf{r}, t)$ ($n_{\mathbf{k}, \sigma}(\mathbf{r}, t)$) with the rate 2γ ($2\gamma_{\sigma}$), where $\gamma = (\gamma_e + \gamma_h)/2$. $L_{\mathbf{k}, \mathbf{k}'}(\mathbf{r}, t)$ and $I_{\mathbf{k}, \sigma}(\mathbf{r}, t)$ in Eqs. (1) and (2), determined microscopically from the self-energy $\hat{\Sigma}$ and the Green’s function \hat{G} in the Nambu-Keldysh formalism (see the Supplemental Material [49] for their explicit form), describe many-body effects, such as band renormalization and collision, as well as the electron-hole pumping and its thermalization.

The electron-hole dynamics is coupled to the dynamics of the coherent cavity-photon amplitude, given by the Heisenberg equation [49],

$$i\hbar\partial_t \lambda_{\text{cav}}(\mathbf{r}, t) = \langle [a(\mathbf{r}, t), H] \rangle = \left[\hbar\omega_{\text{cav}} - \frac{\hbar^2 \nabla^2}{2m_{\text{cav}}} - i\kappa \right] \lambda_{\text{cav}}(\mathbf{r}, t) + g \sum_{\mathbf{k}} p_{\mathbf{k}}(\mathbf{r}, t), \quad (3)$$

where $\hbar\omega_{\text{cav}}$ is the cavity-photon energy, and m_{cav} is a cavity-photon mass.

We consider a uniform steady state given by the ansatz [29–33, 45, 53, 55] $\lambda_{\text{cav}}(t) = \lambda_{\text{cav}}^0 e^{-iEt/\hbar}$, $p_{\mathbf{k}}(t) = p_{\mathbf{k}}^0 e^{-iEt/\hbar}$, where E is the condensate emission energy.

Our discussion assumes that Eqs. (1)–(3) are solved self-consistently for a given parameter set [51]. Defining a complex quantity λ_{eh}^0 [52] by $p_{\mathbf{k}}^0 \equiv \lambda_{\text{eh}}^0 \phi_{\mathbf{k}}$, with $\sum_{\mathbf{k}} |\phi_{\mathbf{k}}|^2 = 1$ and $\text{Arg}[\sum_{\mathbf{k}} \phi_{\mathbf{k}}] = 0$, to quantify the

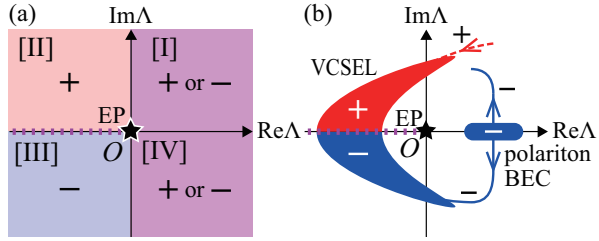


FIG. 3: (Color online) (a) Definition of regions I-IV. In regions II and III, only the “+” or “-”-solution is allowed, respectively. In regions I and IV, both types of solutions may exist. On the dotted line, the solution type switches without being accompanied by discontinuity. (b) Schematic description of how a polariton-BEC evolves to a VCSEL, in terms of Λ . In the evolution, a polariton-BEC exhibits a phase transition (crossover) to a VCSEL when Λ changes counter-clockwise (clockwise) around EP.

electron-hole pair amplitude, we arrive at an eigenvalue problem from Eqs. (1) and (3),

$$\hat{A} \begin{pmatrix} \lambda_{\text{cav}}^0 \\ \lambda_{\text{eh}}^0 \end{pmatrix} = \begin{pmatrix} h_{\text{cav}} & g_0 \\ \tilde{g}_0^* & h_{\text{eh}} \end{pmatrix} \begin{pmatrix} \lambda_{\text{cav}}^0 \\ \lambda_{\text{eh}}^0 \end{pmatrix} = E \begin{pmatrix} \lambda_{\text{cav}}^0 \\ \lambda_{\text{eh}}^0 \end{pmatrix}, \quad (4)$$

where $h_{\text{cav}} = \hbar\omega_{\text{cav}} - i\kappa$, $g_0 = g \sum_{\mathbf{k}} \phi_{\mathbf{k}} = g\phi(\mathbf{r} = 0)$, $\tilde{g}_0^* = g \sum_{\mathbf{k}, \mathbf{k}'} \phi_{\mathbf{k}}^* L_{\mathbf{k}, \mathbf{k}'}$, and $h_{\text{eh}} = \sum_{\mathbf{k}} [(\varepsilon_{\mathbf{k}, \text{e}} + \varepsilon_{\mathbf{k}, \text{h}} - 2i\gamma)|\phi_{\mathbf{k}}|^2 - \sum_{\mathbf{p}, \mathbf{k}'} V_{\mathbf{k}-\mathbf{p}} \phi_{\mathbf{k}}^* \phi_{\mathbf{p}} L_{\mathbf{k}, \mathbf{k}'}]$. The first line in Eq. (4) is equivalent to Eq. (3) in the steady state, and the second line is obtained by multiplying $\phi_{\mathbf{k}}^*$ to both sides of Eq. (1) and integrating over \mathbf{k} .

The matrix A can be diagonalized with eigenvectors

$$\mathbf{u}_- = \begin{pmatrix} \frac{-\varphi + \Omega}{2} \\ -\tilde{g}_0^* \end{pmatrix}, \quad \mathbf{u}_+ = \begin{pmatrix} g_0 \\ \frac{-\varphi + \Omega}{2} \end{pmatrix}, \quad (5)$$

and corresponding eigenvalues $E_{\pm} = [h_{\text{cav}} + h_{\text{eh}} \pm \Omega]/2$. Here, $\Omega = \sqrt{\varphi^2 + 4\tilde{g}_0^*g_0}$, $\varphi = h_{\text{cav}} - h_{\text{eh}}$, and we take $\text{Re}\Omega \geq 0$ (i.e. $\text{Re}E_+ \geq \text{Re}E_-$) without loss of generality. In the diagonal basis, Eq. (4) reads $\text{diag}(E_-, E_+)(\lambda_-^0, \lambda_+^0)^T = E(\lambda_-^0, \lambda_+^0)^T$, where $(\lambda_-^0, \lambda_+^0)^T = \hat{U}(\lambda_{\text{cav}}^0, \lambda_{\text{eh}}^0)^T$ with $\hat{U}^{-1} = (\mathbf{u}_-, \mathbf{u}_+)$.

Other than a trivial solution $\lambda_-^0 = \lambda_+^0 = 0$ that corresponds to the normal phase, Eq. (4) has two types of solutions. One satisfies $\lambda_-^0 \neq 0$ and $E = E_-$. In this case, $\lambda_+^0 = 0$ is automatically satisfied since $\lambda_+^0 \propto \tilde{g}_0^* \lambda_{\text{cav}}^0 + h_{\text{eh}} \lambda_{\text{eh}}^0 - E \lambda_{\text{eh}}^0 = 0$, where we have used the relation $h_{\text{cav}} + h_{\text{eh}} - 2E = \Omega$ and the second line of Eq. (4). The other type is a solution with $\lambda_+^0 \neq 0$ and $E = E_+$. Similarly to the former case, from $h_{\text{cav}} + h_{\text{eh}} - 2E = -\Omega$ and the first line of Eq. (4), we find $\lambda_-^0 \propto -h_{\text{cav}} \lambda_{\text{cav}}^0 - g_0 \lambda_{\text{eh}}^0 + E \lambda_{\text{cav}}^0 = 0$. Thus, $\lambda_-^0 \neq 0$ and $\lambda_+^0 \neq 0$ cannot be satisfied simultaneously, letting us classify the solutions into two types. From here on, we call the former (latter) the “-” (“+”) solution.

Now we show that a first-order-like phase transition between the two solutions occurs. We examine the exceptional point (EP), where $\Omega = 0$ and \mathbf{u}_+ coalesce such

that \hat{A} only has a single eigenvector, and show that this marks the end of a phase boundary. The proof is presented in the Supplemental Material [49] and we sketch the argument here. Consider the quantity,

$$\Lambda \equiv \Omega^2 = \varphi^2 + 4\tilde{g}_0^*g_0, \quad (6)$$

and divide the complex Λ -plane into the regions I-IV, as shown in Fig. 3(a). As shown in Ref. [49], only the “+” (“−”) solution can be realized in region II(III), due to the constraint of the balanced condensate-gain-and-loss giving real emission energy E . When crossing the dotted line in Fig. 3(a), the solution types switch without discontinuity in the emission energy, leading to a smooth crossover. In contrast, sweeping parameters in a route that encircles the EP and crosses through the coexistence regions IV and I, the solution type must switch discontinuously, resulting in a phase transition, proving the theorem [54].

To make contact between the above general arguments and real physical systems, we explicitly solve for the polariton-BEC and VCSEL in a dilute limit. In the dilute equilibrium limit ($\kappa = 0, \gamma \rightarrow 0^+, n_{\mathbf{k},\sigma} \ll 1$) where the polariton-BEC is realized, Eq. (4) reduces to [49]

$$\hat{A}_{\text{BEC}} = \begin{pmatrix} \hbar\omega_{\text{cav}} & g_{\text{R}} \\ g_{\text{R}}^* & \hbar\omega_{\text{X}} \end{pmatrix}, \quad (7)$$

in the Hartree-Fock-Bogoliubov approximation (HFBA) [31–33, 45], being justified in this limit. In Eq. (7), $\hbar\omega_X = E_g - E_X^{\text{bind}}$ is the exciton energy (E_X^{bind} is the exciton binding energy). $g_R = g\phi_X(\mathbf{r} = 0)$ is the Rabi splitting, where $\phi_X(\mathbf{r})$ is an exciton wave function obeying the Schrodinger equation $\int d\mathbf{r}'[-\delta(\mathbf{r} - \mathbf{r}')\hbar^2\nabla'^2/m_{\text{eh}} - V(\mathbf{r} - \mathbf{r}')] \phi_X(\mathbf{r}') = -E_X^{\text{bind}} \phi_X(\mathbf{r})$. In deriving Eq. (7), we have assumed $g_R \ll E_X^{\text{bind}}$, for simplicity. The eigenvalues are given as $E_{\pm}^{\text{BEC}} = [\hbar\omega_{\text{cav}} + \hbar\omega_X \pm \sqrt{\delta^2 + 4|g_R|^2}]/2$, that are just the lower and upper polariton energies [6] (where $\delta = \hbar\omega_{\text{cav}} - \hbar\omega_X$ is the (conventional) detuning parameter). Comparison of the free energies of the two solutions tells us that the “–” solution always emerges.

When the photon decay rate κ is turned on, a phase transition can occur. In the so-called polariton laser regime, where the gas is dilute enough to maintain the polariton picture, the equation of motion is governed by the driven-dissipative Gross-Pitaevskii (ddGP) equation [49, 56], given by,

$$\hat{A}_{\text{GP}} = \begin{pmatrix} \hbar\omega_{\text{cav}} - i\kappa & g_{\text{R}} \\ g_{\text{R}}^* & \hbar\omega_{\text{X}} + U_{\text{X}}|\lambda_{\text{eh}}^0|^2 + iR_{\text{X}} \end{pmatrix}, \quad (8)$$

where U_X is an exciton-exciton interaction strength and $R_X > 0$ describes the net gain of exciton coherence that feeds the condensate [57], arising microscopically from processes such as stimulated scattering. This gives $E_{\pm}^{\text{GP}} = [\hbar\omega_{\text{cav}} + \hbar\omega_X + U_X|\lambda_{\text{eh}}^0|^2 - i(\kappa - R_X) \pm \Omega_{\text{GP}}]/2$ with

$$\Omega_{\text{GP}} = \sqrt{\tilde{\delta}^2 + 4|g_{\text{R}}|^2 - (\kappa + R_{\text{X}})^2 - 2i\tilde{\delta}(\kappa + R_{\text{X}})}, \quad (9)$$

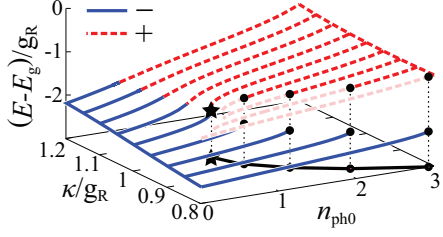


FIG. 4: (Color online) Calculated emission energy E in the case $\hat{A} = \hat{A}_{\text{GP}}$ [Eq. (8)] as a function of the photon decay rate κ/g_R and the (coherent) photon number $n_{\text{ph}}^0 = |\lambda_{\text{cav}}^0|^2$. The solid line projected onto the n_{ph}^0 - κ/g_R plane is a phase boundary. The star represents the exceptional point $\Omega_{\text{GP}} = 0$. We set $\delta/g_R = 0.1$, $\hbar\omega_X/g_R = -2$, $U_X/g_R = 0.1$.

where $\tilde{\delta} = \hbar\omega_{\text{cav}} - (\hbar\omega_X + U_X|\lambda_{\text{eh}}^0|^2)$ is an effective detuning that takes into account the Hartree shift of the exciton component. One can find an EP ($\Omega_{\text{GP}} = 0$) at $\tilde{\delta} = 0$ and $g_R = R_X = \kappa$, giving rise to a phase transition in its vicinity.

We demonstrate this by explicitly solving Eq. (4) when $\hat{A} = \hat{A}_{\text{GP}}$ [Eq. (8)]. Figure 4 shows the calculated condensate emission energy E as a function of the decay rate κ and the coherent photon number $n_{\text{ph}}^0 = |\lambda_{\text{cav}}^0|^2$ (which roughly corresponds to the pump power), in the blue detuning case $\delta/g_R = 0.1$. At $\kappa < g_R$, we find that the “-” solution disappears at a critical value of the pump power, resulting in a phase transition signaled by the discontinuity in the emission energy E . In constructing the phase diagram, we have assumed that we always realize the lowest-energy solution. Relaxing this assumption would shift the position of the phase boundary in detail but not its endpoint. As expected, the phase boundary ends at the EP (where $\kappa = g_R$). When $\kappa > g_R$, the “-” solution crosses over to the “+” solution. The fact that a phase transition arises within the dGP (where the polariton picture still holds) suggests that the second threshold observed in experiments does not necessarily imply a strong-to-weak-coupling transition to a photon laser.

At high pump power where the system operates as a VCSEL, it has been shown within HFBA [31, 32] that Eqs. (1)-(3) reduce to the semiconductor Maxwell-Bloch equations [15], with $L_{\mathbf{k},\mathbf{k}'} = \delta_{\mathbf{k},\mathbf{k}'} N_{\mathbf{k}} = \delta_{\mathbf{k},\mathbf{k}'} (1 - n_{\mathbf{k},\text{e}} - n_{\mathbf{k},\text{h}})$ and

$$\hat{A}_{\text{VL}} = \begin{pmatrix} \hbar\omega_{\text{cav}} - i\kappa & g_0 \\ \tilde{g}_0^{\text{VL}*} & \hbar\omega_{\text{eh}}^{\text{VL}} - 2i\gamma \end{pmatrix}, \quad (10)$$

where $\hbar\omega_{\text{eh}}^{\text{VL}} = \sum_{\mathbf{k}} [(\varepsilon_{\mathbf{k},\text{e}} + \varepsilon_{\mathbf{k},\text{h}})|\phi_{\mathbf{k}}|^2 - \sum_{\mathbf{p}} V_{\mathbf{k}-\mathbf{p}} \phi_{\mathbf{k}}^* \phi_{\mathbf{p}} N_{\mathbf{k}}]$ and $\tilde{g}_0^{\text{VL}*} = g \sum_{\mathbf{k}} \phi_{\mathbf{k}}^* N_{\mathbf{k}}$. A crucial difference compared to the polariton laser case, Eq. (8), is the condensate feeding mechanism. The electron-hole gain $R_X (> 0)$ present in the polariton laser is absent in the VCSEL, since the thermalization process does not work efficiently.

Instead, the condensate is fed by stimulated emission arising from the population inversion $N_{\mathbf{k}} < 0$. The eigenvalues are given by $E_{\pm}^{\text{VL}} = [(\hbar\omega_{\text{cav}} + \hbar\omega_{\text{eh}}^{\text{VL}}) - i(\kappa + 2\gamma) \mp \Omega_{\text{VL}}]/2$ with $\Omega_{\text{VL}} \simeq \sqrt{\delta_{\text{VL}}^2 - 4|g_0|^2 - 2i\delta_{\text{VL}}(\kappa - 2\gamma)}$ (where $\delta_{\text{VL}} = \hbar\omega_{\text{cav}} - \hbar\omega_{\text{eh}}^{\text{VL}}$) [58]. Since the emission energy E needs to be real, $\kappa + 2\gamma \simeq -\text{Im}\Omega_{\text{VL}}$ ($+\text{Im}\Omega_{\text{VL}} > 0$) it is the “+” (“-”) solution that arises for $\text{Im}\Omega_{\text{VL}} > 0$ (< 0).

Figure 3(b) summarizes the above discussion in terms of Λ . Here, the polariton-BEC regime (“-” solution) lies on the real axis $\Lambda_{\text{BEC}} = \delta^2 + |g_R|^2 > 0$, and in depicting the VCSEL regime, we use the property that $\text{Re}\Lambda_{\text{VL}} < 0$ needs to be satisfied when $\text{Im}\Lambda_{\text{VL}} = 0$. Thus, starting from the polariton-BEC with “-” solution, by changing parameters such that Λ evolves clockwise or counter-clockwise around the EP, the system exhibits a crossover or phase transition, respectively, into a VCSEL.

Finally, we return to the schematic phase diagram in terms of the pump power P and the decay rate κ proposed in Fig. 1. Starting from the polariton-BEC ($\kappa = 0$), as the decay rate κ is turned on such that the system turns into a polariton laser, one sees from Eq. (9) that $\text{Im}\Lambda$ increases (decreases) from zero in the case of an effective red (blue) detuning $\tilde{\delta} < 0$ (> 0), where Λ evolves counter-clockwise (clockwise). Since the increasing pump power P usually shifts the effective detuning to red (note that $\tilde{\delta} = \delta - U_X|\lambda_{\text{eh}}^0|^2$), we predict that there always exists a phase boundary between the polariton-BEC and VCSEL in red detuning, $\delta < 0$ [panel (c)]. On the other hand, in blue detuning, $\delta > 0$, $\tilde{\delta}$ may switch its sign to negative when P increases. Depending whether this sign change occurs at a positive or negative $\text{Re}\Lambda$ determines whether the evolution of Λ may reverse to counter-clockwise. Thus, we conjecture that, in the blue detuning case, there exists a phase boundary with an endpoint, as shown in panel (a). On resonance, $\delta = 0$, since we know from Eq. (8) that the EP is at $\kappa = g_R$ in the dilute limit $|\lambda_{\text{eh}}^0| \rightarrow 0$ ($\tilde{\delta} = \delta = 0$), the EP lies on the boundary between the normal and the condensed phase [panel (b)].

Physically, these transition and crossover at different detunings can be understood from the property that the effective red detuning drives the lower (upper)-branch more photonic (excitonic), and vice versa for the blue detuning [6]. This hinders (helps) the lower (upper)-branch condensate to stabilize in the effective red detuning, because the loss from the photonic part becomes larger (smaller) and earns less (more) gain from the excitonic part. This gives rise to the phase transition from “-” to “+”-solution in the red detuning. In contrast, as long as the system stays in the effective blue detuning, it tends to prefer the “-”-solution, to exhibit a crossover.

To summarize, we have shown and demonstrated that the non-Hermitian nature of an electron-hole-photon condensate can give rise to a phase transition. We have shown that the phase boundary may have an endpoint,

in analogy to a liquid-gas phase diagram. The endpoint corresponds to the exceptional point discussed in the context of non-Hermitian quantum mechanics. These conclusions, although derived mainly for microcavity polariton systems, should apply to general driven-dissipative condensates composed of two complex fields.

We thank S. Diehl, D. Myers, S. Mukherjee, M. Yamaguchi, K. Kamide, T. Ogawa, and K. Asano for discussions. This work was supported by KiPAS project in Keio University. RH was supported by a Grand-in-Aid for JSPS fellows (Grant No. 15J02513). YO was supported by Grant-in-Aid for Scientific Research from MEXT and JSPS in Japan (No. JP18K11345, No. JP18H05406, No. JP16K05503). Work at Argonne National Laboratory is supported by the U. S. Department of Energy, Office of Science, BES-MSE under Contract No. DE-AC02-06CH11357.

* Electronic address: hanai@acty.phys.sci.osaka-u.ac.jp

- [1] N. P. Proukakis, D. W. Snoke, and P. B. Littlewood, *Universal Themes of Bose-Einstein Condensation*, (Cambridge University Press, Cambridge, 2017).
- [2] M. H. Anderson, J. R. Ensher, M. R. Matthews, C. E. Wieman, and J. A. Cornell, *Science* **269**, 198 (1995).
- [3] K. B. Davis, M. -O. Mewes, M. R. Andrews, N. J. van Druten, D. S. Durfee, D. M. Kurn, and W. Ketterle, *Phys. Rev. Lett.* **75**, 3969 (1995).
- [4] K. Huang, *Statistical Mechanics 2nd Edition* (Wiley, New York, 1987)
- [5] J. Kasprzak, M. Richard, S. Kundermann, A. Baas, P. Jeambrun, J. Keeling, F. M. Marchetti, M. H. Szymbańska, R. André, J. L. Staehli, V. Savona, P. B. Littlewood, B. Deveaud, and L. S. Dang, *Nature (London)* **443**, 409 (2006).
- [6] H. Deng, H. Haug, Y. Yamamoto, *Rev. Mod. Phys.* **82**, 1489 (2010).
- [7] I. Carusotto and C. Ciuti, *Rev. Mod. Phys.* **85**, 299 (2013).
- [8] T. Byrnes, N. Y. Kim, and Y. Yamamoto, *Nat. Phys.* **10**, 803 (2014).
- [9] Ch. Rüegg, N. Cavadini, A. Furrer, H. -U. Güdel, K. Krämer, H. Mutka, A. Wildes, K. Habicht, and P. Vorderwisch, *Nature* **423** 62 (2003).
- [10] S. O. Demokritov, V. E. Devidov, O. Dzyapko, G. A. Melkov, A. A. Serga, B. Hillebrands, and A. N. Slavin, *Nature (London)* **443**, 430 (2006).
- [11] A. V. Chumak, G. A. Melkov, V. E. Demidov, O. Dzyapko, V. L. Safonov, and S. O. Demokritov, *Phys. Rev. Lett.* **102**, 187205 (2009).
- [12] J. Klaers, J. Schmitt, F. Vewinger, and M. Weitz, *Nature* **468**, 545 (2010).
- [13] T. K. Hakala, A. J. Moilanen, A. I. Väkeväinen, R. Guo, J.-P. Martikainen, K. S. Daskalakis, H. T. Rekola, A. Julku, and P. Törmä, *Nat. Phys.* **14**, 739 (2018).
- [14] M. O. Scully and M. S. Zubairy, *Quantum Optics*, (Cambridge University Press, 1997).
- [15] H. Haug and S. W. Koch, *Quantum Theory of the Optical and Electronic Properties of Semiconductors* (World Scientific, Singapore, 2009).
- [16] A. Imamoglu, R. J. Ram, S. Pau, and Y. Yamamoto, *Phys. Rev. A* **53**, 4250 (1996).
- [17] H. Deng, G. Weihs, D. Snoke, J. Bloch, and Y. Yamamoto, *PNAS* **100**, 15318 (2003).
- [18] D. Bajoni, P. Senellart, E. Wertz, I. Sagnes, A. Miard, A. Lemaître, and J. Bloch, *Phys. Rev. Lett.* **100**, 047401 (2008).
- [19] R. Balili, B. Nelsen, D. W. Snoke, L. Pfeiffer, and K. West, *Phys. Rev. B* **79**, 075319 (2009).
- [20] B. Nelsen, R. Balili, D. W. Snoke, L. Pfeiffer, and K. West, *J. Appl. Phys.* **10**, 122414 (2009).
- [21] J. S. Tempel, F. Veit, M. Aßmann, L. E. Kreilkamp, A. Rahimi-Iman, A. Löffler, S. Höfling, S. Reitzenstein, L. Worschech, A. Forchel, and M. Bayer, *Phys. Rev. B* **85**, 075318 (2012).
- [22] J. S. Tempel, F. Veit, M. Aßmann, L. E. Kreilkamp, S. Höfling, M. Kamp, A. Forchel, and M. Bayer, *New J. Phys.* **14**, 083014 (2012).
- [23] P. Tsotsis, P. S. Eldridge, T. Gao, S. I. Tsintzos, Z. Hatzopoulos, and P. G. Savvidis, *New J. Phys.* **14**, 023060 (2012).
- [24] T. Horikiri, Y. Matsuo, Y. Shikano, A. öffler, S. Höfling, A. Forchel, and Y. Yamamoto, *J. Phys. Soc. Jpn.* **82**, 084709 (2013).
- [25] J. Fischer, S. Brodbeck, A. V. Chernenko, I. Lederer, A. Rahimi-Iman, M. Amthor, V. D. Kulakovskii, L. Worschech, M. Kamp, M. Durnev, C. Schneider, A. V. Kavokin, and S. Höfling, *Phys. Rev. Lett.* **112**, 093902 (2014).
- [26] S. Brodbeck, H. Suchomel, M. Amthor, T. Steinl, M. Kamp, C. Schneider, and S. Höfling, *Phys. Rev. Lett.* **117**, 127401 (2016).
- [27] S. Kim, B. Zhang, Z. Wang, J. Fischer, S. Brodbeck, M. Kamp, C. Schneider, S. Höfling, and H. Deng, *Phys. Rev. X* **6**, 011026 (2016).
- [28] C. P. Dietrich, A. Steude, L. Tropf, M. Schubert, N. M. Kronenberg, K. Ostermann, S. Höfling, and M. C. Gather, *Sci. Adv.* **2**, e160666 (2016).
- [29] M. H. Szymbańska, J. Keeling, and P. B. Littlewood, *Phys. Rev. Lett.* **96**, 230602 (2006).
- [30] M. H. Szymbańska, J. Keeling, and P. B. Littlewood, *Phys. Rev. B* **75**, 195331 (2007).
- [31] M. Yamaguchi, K. Kamide, T. Ogawa, and Y. Yamamoto, *New J. Phys.* **14**, 065001 (2012).
- [32] M. Yamaguchi, K. Kamide, R. Nii, T. Ogawa, and Y. Yamamoto, *Phys. Rev. Lett.* **111**, 026404 (2013).
- [33] M. Yamaguchi, R. Nii, K. Kamide, T. Ogawa, and Y. Yamamoto, *Phys. Rev. B* **91**, 115129 (2015).
- [34] T. Kato, *Perturbation theory of linear operators* (Springer, Berlin, 1966).
- [35] C. M. Bender and S. Boettcher, *Phys. Rev. Lett.* **80**, 5243 (1998).
- [36] W. D. Heiss, *Eur. Phys. J. D.* **7**, 1 (1999).
- [37] C. Dembowski, B. Dietz, H.-D. Gräf, H. L. Harney, A. Heine, W. D. Heiss, and A. Richter, *Phys. Rev. E* **69**, 056216 (2004).
- [38] W. D. Heiss, *J. Phys. A: Math. Theor.* **45**, 444016 (2012).
- [39] C. Dembowski, H.-D. Gräf, H. L. Harney, A. Heine, W. D. Heiss, H. Rehfeld, and A. Richter, *Phys. Rev. Lett.* **86**, 787 (2001).
- [40] S.-B. Lee, J. Yang, S. Moon, S.-Y. Lee, J.-B. Shim, S. W. Kim, J.-H. Lee, and K. An, *Phys. Rev. Lett.* **103**, 134101 (2009).
- [41] T. Gao, E. Estrecho, K. Y. Bliokh, T. C. H. Liew, M. D.

Fraser, S. Brodbeck, M. Kamp, C. Schneider, S. Höfling, Y. Yamamoto, F. Nori, Y. S. Kivshar, A. G. Truscott, R. G. Dall, and E. A. Ostrovskaya, *Nature* **526** 22 (2015).

[42] E. Graefe, *J. Phys. A: Math. Theor.* **45**, 444015 (2012).

[43] H. Cartarius and G. Wunner, *Phys. Rev. A* **86**, 013612 (2012).

[44] D. Dast, D. Haag, H. Cartarius, G. Wunner, R. Eichler, and J. Main, *Fortschr. Phys.* **61**, 124 (2013).

[45] R. Hanai, P. B. Littlewood, and Y. Ohashi, *Phys. Rev. B* **97**, 245302 (2018).

[46] M. Aßmann, J. Tempel, F. Veit, M. Bayer, A. Rahimi-Iman, A. Löffler, S. Höfling, S. Reitzenstein, L. Worschech, and A. Forchel, *PNAS* **108**, 1804 (2011).

[47] M. Nakayama, K. Murakami, and D. Kim, *J. Phys. Soc. Jpn.* **85**, 054702 (2016).

[48] M. Nakayama and M. Ueda, *Phys. Rev. B* **95**, 125315 (2017).

[49] See the Supplemental Material for details.

[50] J. Rammer, *Quantum Field Theory of Non-Equilibrium States* (Cambridge University Press, Cambridge, 2007).

[51] Precisely speaking, we solve the Dyson's equation (where its explicit form is given in the Supplemental Material) to obtain all the terms in Eqs. (1)-(3).

[52] C. Comte and P. Nozières, *J. Physique* **43**, 1069 (1982).

[53] R. Hanai, P. B. Littlewood, and Y. Ohashi, *Phys. Rev. B* **96**, 125206 (2017).

[54] We have implicitly assumed that \hat{A} is a smooth function of the input parameters.

[55] R. Hanai, P. B. Littlewood, and Y. Ohashi, *J. Low Temp. Phys.* **183**, 127 (2016).

[56] M. Wouters and I. Carusotto, *Phys. Rev. Lett.* **99**, 140402 (2007).

[57] The nonlinearity and the gain is present only in the diagonal exciton component under the condition $g_R \ll E_X^{\text{bind}}$ [49].

[58] Here, we have assumed that the VCSEL is in an extremely strong pumping regime where a large population inversion $N_{\mathbf{k}} \simeq -1$ exists at predominant momentum window, which makes $\hbar\omega_{\text{eh}}^{\text{VL}} \simeq \sum_{\mathbf{k}} [(\varepsilon_{\mathbf{k},e} + \varepsilon_{\mathbf{k},h})|\phi_{\mathbf{k}}|^2 + \sum_{\mathbf{p}} V_{\mathbf{k}-\mathbf{p}} \phi_{\mathbf{k}}^* \phi_{\mathbf{p}}]$ real number and $\tilde{g}_0^{\text{VL}*} \simeq -g_0^* < 0$.

Supplemental Material for “Non-Hermitian phase transition from a polariton Bose-Einstein condensate to a photon laser”

MODEL

We provide here the explicit form of the Hamiltonian H of our model, depicted schematically in Fig. 1 in the main text [1–4]. The Hamiltonian is given by the sum of three parts $H = H_s + H_{\text{env}} + H_t$. Here,

$$H_s = \sum_{\mathbf{k}, \sigma=e,h} \varepsilon_{\mathbf{k}, \sigma} c_{\mathbf{k}, \sigma}^\dagger c_{\mathbf{k}, \sigma} + \sum_{\mathbf{q}} \varepsilon_{\mathbf{q}}^{\text{cav}} a_{\mathbf{q}}^\dagger a_{\mathbf{q}} + \sum_{\mathbf{k}, \mathbf{k}', \mathbf{q}} V_{\mathbf{k}-\mathbf{k}'} \\ \times \left[\sum_{\sigma=e,h} c_{\mathbf{k}+\mathbf{q}/2, \sigma}^\dagger c_{-\mathbf{k}+\mathbf{q}/2, \sigma}^\dagger c_{-\mathbf{k}'+\mathbf{q}/2, \sigma} c_{\mathbf{k}'+\mathbf{q}/2, \sigma} \right. \\ \left. - c_{\mathbf{k}+\mathbf{q}/2, e}^\dagger c_{-\mathbf{k}+\mathbf{q}/2, h}^\dagger c_{-\mathbf{k}'+\mathbf{q}/2, h} c_{\mathbf{k}'+\mathbf{q}/2, e} \right] \\ + \sum_{\mathbf{k}, \mathbf{q}} [g c_{\mathbf{p}+\mathbf{q}/2, e}^\dagger c_{-\mathbf{k}+\mathbf{q}/2, h}^\dagger a_{\mathbf{q}} + \text{h.c.}], \quad (\text{S1})$$

is the system Hamiltonian composed of electrons, holes, and photons. $c_{\mathbf{p}, e(h)}$ is an annihilation operator of an electron (hole) and $\varepsilon_{\mathbf{p}, e(h)} = \hbar^2 \mathbf{p}^2 / (2m_{e(h)}) + E_g/2$ is the kinetic energy of an electron (hole), where $m_{e(h)}$ is the effective mass of an electron (hole) in the conduction (valence) band and E_g is the energy gap of the material. $a_{\mathbf{q}}$ is an annihilation operator of a photon in the cavity, and $\varepsilon_{\mathbf{q}}^{\text{cav}} = \hbar\omega_{\text{cav}} + \hbar^2 \mathbf{q}^2 / (2m_{\text{cav}})$ is the kinetic energy of photons, where $\hbar\omega_{\text{cav}} = (c/n_c)\hbar(2\pi/\lambda)$ can be controlled by varying the microcavity length λ (n_c is the refractive index of the microcavity). The second term describes the pair-annihilation (creation) of electrons and holes accompanied by creation (annihilation) of photons, where g is the dipole coupling constant. The last term describes the repulsive and attractive Coulomb interactions between the electrons and holes, where $V_{\mathbf{k}-\mathbf{k}'} = e^2 / (2\epsilon|\mathbf{k} - \mathbf{k}'|)$ (ϵ is the dielectric constant).

Incoherent pumping of electrons and holes is modeled as a coupling to a (free) bath via the tunneling coefficient $\Gamma_{b,e(h)}$. Similarly, we model the photon decay as a coupling to a (free) vacuum via Γ_v . These are described by the Hamiltonian,

$$H_t = \sum_{\mathbf{k}, \mathbf{K}, \sigma=e,h,i} [\Gamma_{b,\sigma} c_{\mathbf{k}, \sigma}^\dagger b_{\mathbf{K}, \sigma} e^{i\mathbf{k} \cdot \mathbf{r}_i} e^{-i\mathbf{K} \cdot \mathbf{R}_i} + \text{h.c.}] \\ + \sum_{\mathbf{q}, \mathbf{Q}, i} [\Gamma_v a_{\mathbf{q}}^\dagger \psi_{\mathbf{Q}} e^{i\mathbf{q} \cdot \mathbf{r}_i} e^{-i\mathbf{Q} \cdot \mathbf{R}_i} + \text{h.c.}], \quad (\text{S2})$$

$$H_{\text{env}} = \sum_{\mathbf{P}, \sigma=e,h} \varepsilon_{\mathbf{P}, \sigma}^b b_{\mathbf{P}, \sigma}^\dagger b_{\mathbf{P}, \sigma} + \sum_{\mathbf{Q}} \varepsilon_{\mathbf{Q}}^{\text{ph}, v} \psi_{\mathbf{Q}}^\dagger \psi_{\mathbf{Q}}. \quad (\text{S3})$$

Here, $b_{\mathbf{P}, e(h)}$ and $\psi_{\mathbf{Q}}$ are annihilation operators of the bath electrons (holes) and the vacuum photons, respectively, and $\varepsilon_{\mathbf{P}, e(h)}^b$ and $\varepsilon_{\mathbf{Q}}^v$ are the kinetic energy of the bath electrons (holes) and the vacuum photons, respectively. We have assumed that the carriers tunnel from position \mathbf{r}_i in the system to \mathbf{R}_i in the bath or vacuum ($i = 1, 2, \dots, N_t$). The positions \mathbf{r}_i and \mathbf{R}_i are assumed to be randomly distributed, in order to model homogeneous pumping and decay of carriers [1]. As shown soon later, this results in a decay rate of photons given by

$$\kappa = \pi N_t |\Gamma_v|^2 \rho_v, \quad (\text{S4})$$

and an incoherent pumping rate of the electrons (holes)

$$\gamma_{e(h)} = \pi N_t |\Gamma_{b,e(h)}|^2 \rho_{b,e(h)}. \quad (\text{S5})$$

Here, the bath electron (hole) density of states $\rho_{b,e(h)}$ and the vacuum photon density of states ρ_v are both assumed to be white (i.e., $\rho_v = \text{const.}, \rho_{b,\sigma=e,h} = \text{const.}$).

For the system to converge into a steady state, we assume that the bath and the vacuum are large compared to the system such that they stay in equilibrium. The bath electron and hole distribution is given by the Fermi distribution function,

$$f_{b,\sigma=e,h}(\omega) = \frac{1}{e^{(\hbar\omega - \mu_{b,\sigma})/T_b} + 1}, \quad (\text{S6})$$

characterized by the bath temperature T_b and the electron and hole chemical potential $\mu_{b,\sigma=e,h}$. The vacuum photon distribution is given by, $f_v(\omega) = 0$.

DERIVATION OF THE EQUATION OF MOTION

We now derive the (exact) equation of motion of the above model, given by the generalized Boltzmann equations [Eqs. (1) and (2) in the main text] and the Heisenberg equation of the photon amplitude [Eq. (3) in the main text]. Let us first derive the former. To study the dynamics of an interacting many-body system, it is convenient to consider the Nambu-Keldysh single-particle Green's function of electrons and holes, defined by [5],

$$\hat{G}_{\alpha, \beta}(\mathbf{r}_1, t_1; \mathbf{r}_2, t_2) = \begin{pmatrix} \hat{G}^R(\mathbf{r}_1, t_1; \mathbf{r}_2, t_2) & \hat{G}^K(\mathbf{r}_1, t_1; \mathbf{r}_2, t_2) \\ 0 & \hat{G}^A(\mathbf{r}_1, t_1; \mathbf{r}_2, t_2) \end{pmatrix}_{\alpha, \beta}$$

$$= -\frac{i}{\hbar} \begin{pmatrix} \theta(t_1 - t_2) \langle \{\hat{\Psi}(\mathbf{r}_1, t_1) \diamond \hat{\Psi}^\dagger(\mathbf{r}_2, t_2)\} \rangle & \langle \hat{\Psi}(\mathbf{r}_1, t_1) \diamond \hat{\Psi}^\dagger(\mathbf{r}_2, t_2) - \hat{\Psi}^\dagger(\mathbf{r}_2, t_2) \diamond \hat{\Psi}(\mathbf{r}_1, t_1) \rangle \\ 0 & -\theta(t_2 - t_1) \langle \{\hat{\Psi}(\mathbf{r}_1, t_1) \diamond \hat{\Psi}^\dagger(\mathbf{r}_2, t_2)\} \rangle \end{pmatrix}_{\alpha, \beta}, \quad (\text{S7})$$

where $\theta(x)$ is a step function. Here, we have introduced a Nambu operator

$$\hat{\Psi}(\mathbf{r}, t) = \begin{pmatrix} c_e(\mathbf{r}, t) \\ c_h^\dagger(\mathbf{r}, t) \end{pmatrix} \equiv \begin{pmatrix} \Psi_1(\mathbf{r}, t) \\ \Psi_2(\mathbf{r}, t) \end{pmatrix}, \quad (\text{S8})$$

and the product

$$(\hat{\Psi}(\mathbf{r}_1, t_1) \diamond \hat{\Psi}^\dagger(\mathbf{r}_2, t_2))_{s, s'} \equiv \Psi_s(\mathbf{r}_1, t_1) \Psi_{s'}^\dagger(\mathbf{r}_2, t_2) = \begin{pmatrix} c_e(\mathbf{r}_1, t_1) c_e^\dagger(\mathbf{r}_2, t_2) & c_e(\mathbf{r}_1, t_1) c_h(\mathbf{r}_2, t_2) \\ c_h^\dagger(\mathbf{r}_1, t_1) c_e^\dagger(\mathbf{r}_2, t_2) & c_h^\dagger(\mathbf{r}_1, t_1) c_h(\mathbf{r}_2, t_2) \end{pmatrix}_{s, s'}, \quad (\text{S9})$$

$$(\hat{\Psi}^\dagger(\mathbf{r}_2, t_2) \diamond \hat{\Psi}(\mathbf{r}_1, t_1))_{s, s'} \equiv \Psi_{s'}^\dagger(\mathbf{r}_2, t_2) \Psi_s(\mathbf{r}_1, t_1) = \begin{pmatrix} c_e^\dagger(\mathbf{r}_2, t_2) c_e(\mathbf{r}_1, t_1) & c_h(\mathbf{r}_2, t_2) c_e(\mathbf{r}_1, t_1) \\ c_e^\dagger(\mathbf{r}_2, t_2) c_h^\dagger(\mathbf{r}_1, t_1) & c_h(\mathbf{r}_2, t_2) c_h^\dagger(\mathbf{r}_1, t_1) \end{pmatrix}_{s, s'}. \quad (\text{S10})$$

An especially important quantity of interest is the lesser Green's function,

$$\begin{aligned} \hat{G}^<(\mathbf{r}_1, t_1; \mathbf{r}_2, t_2) &= \frac{1}{2} [-\hat{G}^R + \hat{G}^A + \hat{G}^K](\mathbf{r}_1, t_1; \mathbf{r}_2, t_2) = \frac{i}{\hbar} \langle \hat{\Psi}^\dagger(\mathbf{r}_2, t_2) \diamond \hat{\Psi}(\mathbf{r}_1, t_1) \rangle \\ &= \frac{i}{\hbar} \begin{pmatrix} \langle c_e^\dagger(\mathbf{r}_2, t_2) c_e(\mathbf{r}_1, t_1) \rangle & \langle c_h(\mathbf{r}_2, t_2) c_e(\mathbf{r}_1, t_1) \rangle \\ \langle c_e^\dagger(\mathbf{r}_2, t_2) c_h^\dagger(\mathbf{r}_1, t_1) \rangle & \langle c_h(\mathbf{r}_2, t_2) c_h^\dagger(\mathbf{r}_1, t_1) \rangle \end{pmatrix}, \end{aligned} \quad (\text{S11})$$

which directly relates to the electron (hole) density $n_{\mathbf{k}, e(h)}(\mathbf{r}, t)$ and the polarization $p_{\mathbf{k}}(\mathbf{r}, t)$. By transforming this quantity to the so-called Wigner representation, where the coordinates (\mathbf{r}_1, t_1) and (\mathbf{r}_2, t_2) are rewritten in terms of the relative coordinate $\mathbf{r}_r = \mathbf{r}_1 - \mathbf{r}_2$, $t_r = t_1 - t_2$ and the center of motion coordinate $\mathbf{r} = (\mathbf{r}_1 + \mathbf{r}_2)/2$, $t = (t_1 + t_2)/2$, $n_{\mathbf{k}, \sigma=e,h}(\mathbf{r}, t)$ and $p_{\mathbf{k}}(\mathbf{r}, t)$ are obtained as,

$$\begin{pmatrix} n_{\mathbf{k}, e}(\mathbf{r}, t) & p_{\mathbf{k}}(\mathbf{r}, t) \\ p_{\mathbf{k}}^*(\mathbf{r}, t) & 1 - n_{\mathbf{k}, h}(\mathbf{r}, t) \end{pmatrix} = -i\hbar \int d\mathbf{r}_r e^{-i\mathbf{k} \cdot \mathbf{r}_r} \hat{G}^<(\mathbf{r}_r, t_r = 0; \mathbf{r}, t) = -i\hbar \int_{-\infty}^{\infty} \frac{d\omega}{2\pi} \hat{G}^<(\mathbf{k}, \omega; \mathbf{r}, t). \quad (\text{S12})$$

Below, we show that the equation of motion of these valuables are given by the generalized Boltzmann equations (1) and (2).

The dynamics of the single-particle Green's function \hat{G} is determined by the Dyson's equation [5],

$$\hat{G}_{\alpha, \beta} = \hat{G}_{\alpha, \beta}^0 + \hat{G}_{\alpha, \alpha'}^0 \otimes \hat{\Sigma}_{\alpha', \beta'} \otimes \hat{G}_{\beta', \beta}, \quad (\text{S13})$$

where we have introduced a short-hand notation,

$$[\hat{A} \otimes \hat{B}](\mathbf{r}_1, t_1; \mathbf{r}_2, t_2) = \int_{-\infty}^{\infty} dt'_1 \int d\mathbf{r}'_1 \hat{A}(\mathbf{r}_1, t_1; \mathbf{r}'_1, t'_1) \hat{B}(\mathbf{r}'_1, t'_1; \mathbf{r}_2, t_2), \quad (\text{S14})$$

and have omitted the space-time index in Eq. (S13). The (Fourier transformed) free electron-hole Green's function is given by,

$$\hat{G}_0(\mathbf{k}, \omega) = \begin{pmatrix} \hat{G}_0^R(\mathbf{k}, \omega) & \hat{G}_0^K(\mathbf{k}, \omega) \\ 0 & \hat{G}_0^A(\mathbf{k}, \omega) \end{pmatrix} \quad (\text{S15})$$

with

$$G_0^R(\mathbf{k}, \omega) = \begin{pmatrix} \hbar\omega + i\delta - \varepsilon_{\mathbf{k}, e} & 0 \\ 0 & \hbar\omega + i\delta + \varepsilon_{\mathbf{k}, h} \end{pmatrix}^{-1}, \quad (\text{S16})$$

$$G_0^A(\mathbf{k}, \omega) = \begin{pmatrix} \hbar\omega - i\delta - \varepsilon_{\mathbf{k}, e} & 0 \\ 0 & \hbar\omega - i\delta + \varepsilon_{\mathbf{k}, h} \end{pmatrix}^{-1}, \quad (\text{S17})$$

$$G_0^K(\mathbf{k}, \omega) = \begin{pmatrix} -2\pi i [1 - 2f(\omega)] \delta(\hbar\omega - \varepsilon_{\mathbf{k}, e}) & 0 \\ 0 & 2\pi i [1 - 2f(-\omega)] \delta(\hbar\omega + \varepsilon_{\mathbf{k}, h}) \end{pmatrix}, \quad (\text{S18})$$

where $\tau_{i=1,2,3}$ are Pauli matrices acting on the Nambu space. Here, $f(\omega)$ in the Keldysh component is the initial distribution of the relevant system, which, as shown below, does not affect the final form of the equation of motion. The effects of the many-body interaction and the coupling to the bath are described by the self-energy,

$$\hat{\Sigma}(\mathbf{r}_1, t_1; \mathbf{r}_2, t_2) = \begin{pmatrix} \hat{\Sigma}^R(\mathbf{r}_1, t_1; \mathbf{r}_2, t_2) & \hat{\Sigma}^K(\mathbf{r}_1, t_1; \mathbf{r}_2, t_2) \\ 0 & \hat{\Sigma}^A(\mathbf{r}_1, t_1; \mathbf{r}_2, t_2) \end{pmatrix}. \quad (\text{S19})$$

We can proceed by formally solving the Dyson's equation (S13) as,

$$\hat{G}^R = [[G_0^R]^{-1} - \hat{\Sigma}^R]^{-1}, \quad (\text{S20})$$

$$\hat{G}^A = [[G_0^A]^{-1} - \hat{\Sigma}^A]^{-1} = [\hat{G}^R]^\dagger, \quad (\text{S21})$$

$$\begin{aligned} \hat{G}^K &= \hat{G}^R \otimes \hat{\Sigma}^K \otimes \hat{G}^A + (1 + \hat{G}^R \otimes \hat{\Sigma}^R) \hat{G}_0^K (1 + \hat{\Sigma}^A \otimes \hat{G}^A) \\ &= \hat{G}^R \otimes \hat{\Sigma}^K \otimes \hat{G}^A + \hat{G}^R \otimes [\hat{G}_0^R]^{-1} \otimes \hat{G}_0^K \otimes [\hat{G}_0^A]^{-1} \otimes \hat{G}^A \\ &= \hat{G}^R \otimes \hat{\Sigma}^K \otimes \hat{G}^A. \end{aligned} \quad (\text{S22})$$

In deriving Eq. (S22), we have used Eqs. (S20) and (S21) in the second equality and have used the relation,

$$[[\hat{G}_0^R]^{-1} \otimes \hat{G}_0^K \otimes [\hat{G}_0^A]^{-1}](\mathbf{k}, \omega) = [\hat{G}_0^R]^{-1}(\mathbf{k}, \omega) \hat{G}_0^K(\mathbf{k}, \omega) [\hat{G}_0^A]^{-1}(\mathbf{k}, \omega) = 0, \quad (\text{S23})$$

in the third. From Eq. (S22), the lesser Green's function $\hat{G}^<$ satisfies,

$$\begin{aligned} 0 &= [\hat{G}^R - \hat{G}^A + \hat{G}^<] - \hat{G}^R \otimes [\hat{\Sigma}^R - \hat{\Sigma}^A + \hat{\Sigma}^<] \otimes \hat{G}^A \\ &= \hat{G}^R \otimes [1 + \hat{\Sigma}^A \otimes G^A] - [1 + \hat{G}^R \otimes \hat{\Sigma}^R] \otimes \hat{G}^A + \hat{G}^< - \hat{G}^R \otimes \hat{\Sigma}^< \otimes G^A \\ &= [\hat{G}^R \otimes [\hat{G}_0^A]^{-1} \otimes \hat{G}^A - \hat{G}^R \otimes [\hat{G}_0^R]^{-1} \otimes \hat{G}^A] + [\hat{G}^< - \hat{G}^R \otimes \hat{\Sigma}^< \otimes \hat{G}^A] = \hat{G}^< - \hat{G}^R \otimes \hat{\Sigma}^< \otimes \hat{G}^A, \end{aligned} \quad (\text{S24})$$

or

$$\hat{G}^< = \hat{G}^R \otimes \hat{\Sigma}^< \otimes \hat{G}^A, \quad (\text{S25})$$

where

$$\hat{\Sigma}^< = \frac{1}{2}[-\hat{\Sigma}^R + \hat{\Sigma}^A + \hat{\Sigma}^K], \quad (\text{S26})$$

is the lesser component of the self-energy. We have used Eqs. (S20) and (S21) in obtaining the third equality of Eq. (S24) and $[\hat{G}_0^R]^{-1} = [\hat{G}_0^A]^{-1}$ in the last. This yields,

$$[\hat{G}_0^R]^{-1} \otimes \hat{G}^< = \hat{\Sigma}^R \otimes \hat{G}^< + \hat{\Sigma}^< \otimes \hat{G}^A, \quad (\text{S27})$$

$$\hat{G}^< \otimes [\hat{G}_0^A]^{-1} = \hat{G}^< \otimes \hat{\Sigma}^A + \hat{G}^R \otimes \hat{\Sigma}^<, \quad (\text{S28})$$

giving,

$$-[\hat{G}_0^R]^{-1} \otimes \hat{G}^< + \hat{G}^< \otimes [\hat{G}_0^A]^{-1} = -\hat{\Sigma}^R \otimes \hat{G}^< + \hat{G}^< \otimes \hat{\Sigma}^A - \hat{\Sigma}^< \otimes \hat{G}^A + \hat{G}^R \otimes \hat{\Sigma}^<. \quad (\text{S29})$$

Let us obtain the explicit form of Eq. (S29). The two terms on the left-hand side is written as,

$$[[\hat{G}_0^R]^{-1} \otimes \hat{G}^<](\mathbf{r}_1, t_1; \mathbf{r}_2, t_2) = \begin{pmatrix} i\hbar \frac{\vec{\partial}}{\partial t_1} - \left(-\frac{\hbar^2 \vec{\nabla}_1^2}{2m_e} + \frac{E_g}{2} \right) & 0 \\ 0 & i\hbar \frac{\vec{\partial}}{\partial t_1} + \left(-\frac{\hbar^2 \vec{\nabla}_1^2}{2m_h} + \frac{E_g}{2} \right) \end{pmatrix} \hat{G}^<(\mathbf{r}_1, t_1; \mathbf{r}_2, t_2), \quad (\text{S30})$$

$$[\hat{G}^< \otimes [\hat{G}_0^A]^{-1}](\mathbf{r}_1, t_1; \mathbf{r}_2, t_2) = \hat{G}^<(\mathbf{r}_1, t_1; \mathbf{r}_2, t_2) \begin{pmatrix} i\hbar \frac{\vec{\partial}}{\partial t_2} - \left(-\frac{\hbar^2 \vec{\nabla}_2^2}{2m_e} + \frac{E_g}{2} \right) & 0 \\ 0 & i\hbar \frac{\vec{\partial}}{\partial t_2} + \left(-\frac{\hbar^2 \vec{\nabla}_2^2}{2m_h} + \frac{E_g}{2} \right) \end{pmatrix}, \quad (\text{S31})$$

where the partial derivatives with arrows pointing to the right (left) operates to the quantity on the right (left). In the Wigner representation, Eqs. (S30) and (S31) are expressed as,

$$[[\hat{G}_0^R]^{-1} \otimes \hat{G}^<](\mathbf{k}, \omega; \mathbf{r}, t)$$

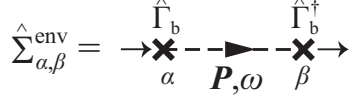


FIG. S1: (Color online) Diagrammatic expression $\hat{\Sigma}_{\text{env}}$. The dashed line represents the bath Green's function \hat{B}_b and the cross represents $\hat{\Gamma}_b$.

$$= \begin{pmatrix} \frac{i\hbar}{2} \frac{\vec{\partial}}{\partial t} + \hbar\omega - \left[-\frac{\hbar^2}{2m_e} \left(\frac{\vec{\nabla}}{2} + i\mathbf{k} \right)^2 + \frac{E_g}{2} \right] & 0 \\ 0 & \frac{i\hbar}{2} \frac{\vec{\partial}}{\partial t} + \hbar\omega + \left[-\frac{\hbar^2}{2m_h} \left(\frac{\vec{\nabla}}{2} + i\mathbf{k} \right)^2 + \frac{E_g}{2} \right] \end{pmatrix} \hat{G}^<(\mathbf{k}, \omega; \mathbf{r}, t), \quad (\text{S32})$$

$$= \hat{G}^<(\mathbf{k}, \omega; \mathbf{r}, t) \begin{pmatrix} -\frac{i\hbar}{2} \frac{\vec{\partial}}{\partial t} + \hbar\omega - \left[-\frac{\hbar^2}{2m_e} \left(\frac{\vec{\nabla}}{2} - i\mathbf{k} \right)^2 + \frac{E_g}{2} \right] & 0 \\ 0 & -\frac{i\hbar}{2} \frac{\vec{\partial}}{\partial t} + \hbar\omega + \left[-\frac{\hbar^2}{2m_h} \left(\frac{\vec{\nabla}}{2} - i\mathbf{k} \right)^2 + \frac{E_g}{2} \right] \end{pmatrix} \quad (\text{S33})$$

Integrating both sides of Eq. (S29) over ω , we obtain the generalized Boltzmann equation,

$$\begin{pmatrix} \frac{\partial}{\partial t} n_{\mathbf{k},e}(\mathbf{r}, t) + \mathbf{v}_{\mathbf{k},e} \cdot \nabla n_{\mathbf{k},e}(\mathbf{r}, t) & \frac{\partial}{\partial t} p_{\mathbf{k}}(\mathbf{r}, t) + \frac{i}{\hbar} (\varepsilon_{\mathbf{k},e} + \varepsilon_{\mathbf{k},h} - \frac{\hbar^2 \nabla^2}{4m_{\text{eh}}}) p_{\mathbf{k}}(\mathbf{r}, t) \\ \frac{\partial}{\partial t} p_{\mathbf{k}}^*(\mathbf{r}, t) - \frac{i}{\hbar} (\varepsilon_{\mathbf{k},e} + \varepsilon_{\mathbf{k},h} - \frac{\hbar^2 \nabla^2}{4m_{\text{eh}}}) p_{\mathbf{k}}^*(\mathbf{r}, t) & -\frac{\partial}{\partial t} n_{\mathbf{k},h}(\mathbf{r}, t) - \mathbf{v}_{\mathbf{k},h} \cdot \nabla n_{\mathbf{k},h}(\mathbf{r}, t) \end{pmatrix} \\ = \int_{-\infty}^{\infty} \frac{d\omega}{2\pi} [-\hat{\Sigma}^R \otimes \hat{G}^< + \hat{G}^< \otimes \hat{\Sigma}^A - \hat{\Sigma}^< \otimes \hat{G}^A + \hat{G}^R \otimes \hat{\Sigma}^<](\mathbf{k}, \omega; \mathbf{r}, t), \quad (\text{S34})$$

where $2m_{\text{eh}}^{-1} = m_e^{-1} + m_h^{-1}$ is twice the reduced mass. The right-hand side can be interpreted as the collision term. Note that, unlike in the conventional Boltzmann equation, the collision term depends explicitly on time and space.

To show that the coupling to the bath induces dephasing and decay, we separate the self-energy into two terms,

$$\hat{\Sigma} = \hat{\Sigma}_{\text{env}} + \hat{\Sigma}_{\text{int}}, \quad (\text{S35})$$

where the first term ($\hat{\Sigma}_{\text{env}}$) describes the effects from the system-bath coupling and the second term ($\hat{\Sigma}_{\text{int}}$) describes the many-body interaction effects. We note that the cross-term $\hat{\Sigma}_{\text{env-int}}$ is absent since we have assumed that the bath is large compared to the system. The diagrammatic expression of $\hat{\Sigma}_{\text{env}}$ is shown in Fig. S1, where its explicit form is given by,

$$\hat{\Sigma}_{\text{env}}^R(\mathbf{k}, \omega; \mathbf{r}, t) = \hat{\Sigma}_{\text{env}}^R = N_t \sum_{\mathbf{P}} \hat{\Gamma}_b^\dagger \hat{B}_b^R(\mathbf{P}, \omega) \hat{\Gamma}_b = \begin{pmatrix} -i\gamma_e & 0 \\ 0 & -i\gamma_h \end{pmatrix}, \quad (\text{S36})$$

$$\hat{\Sigma}_{\text{env}}^A(\mathbf{k}, \omega; \mathbf{r}, t) = \hat{\Sigma}_{\text{env}}^A = N_t \sum_{\mathbf{P}} \hat{\Gamma}_b^\dagger \hat{B}_b^A(\mathbf{P}, \omega) \hat{\Gamma}_b = \begin{pmatrix} i\gamma_e & 0 \\ 0 & i\gamma_h \end{pmatrix}, \quad (\text{S37})$$

$$\hat{\Sigma}_{\text{env}}^K(\mathbf{k}, \omega; \mathbf{r}, t) = \hat{\Sigma}_{\text{env}}^K(\omega) = N_t \sum_{\mathbf{P}} \hat{\Gamma}_b^\dagger \hat{B}_b^K(\mathbf{P}, \omega) \hat{\Gamma}_b = \begin{pmatrix} 2i\gamma_e[1 - 2f_{b,e}(\omega)] & 0 \\ 0 & -2i\gamma_h[1 - 2f_{b,h}(-\omega)] \end{pmatrix}, \quad (\text{S38})$$

and the lesser component is given by,

$$\hat{\Sigma}_{\text{env}}^<(\omega) = 2i \begin{pmatrix} \gamma_e f_{b,e}(\omega) & 0 \\ 0 & \gamma_h f_{b,h}(-\omega) \end{pmatrix}. \quad (\text{S39})$$

Here, $\hat{\Gamma}_b = \text{diag}(\Gamma_{b,e}, \Gamma_{b,h})$ and

$$\hat{B}_b^R(\mathbf{k}, \omega) = \begin{pmatrix} \hbar\omega + i\delta - \varepsilon_{\mathbf{k},e}^b & 0 \\ 0 & \hbar\omega + i\delta + \varepsilon_{\mathbf{k},h}^b \end{pmatrix}^{-1}, \quad (\text{S40})$$

$$\hat{B}_b^A(\mathbf{k}, \omega) = \begin{pmatrix} \hbar\omega - i\delta - \varepsilon_{\mathbf{k},e}^b & 0 \\ 0 & \hbar\omega - i\delta + \varepsilon_{\mathbf{k},h}^b \end{pmatrix}^{-1}, \quad (\text{S41})$$

$$\hat{B}_b^K(\mathbf{k}, \omega) = \begin{pmatrix} -2\pi i[1 - 2f_{b,e}(\omega)]\delta(\hbar\omega - \varepsilon_{\mathbf{k},e}^b) & 0 \\ 0 & 2\pi i[1 - 2f_{b,h}(-\omega)]\delta(\hbar\omega + \varepsilon_{\mathbf{k},h}^b) \end{pmatrix}, \quad (\text{S42})$$

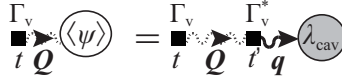


FIG. S2: (Color online) Diagrammatic expression Eq. (S56). The dotted curved line represents the vacuum photon Green's function B_v^R and the solid square represents the tunneling Γ_v .

is the electron-hole single-particle Green's function in the bath. Since we have assumed that the bath is large compared to the system, the bath Green's function is unaffected by the system dynamics. From Eqs. (S36)-(S39),

$$\begin{aligned} & \int_{-\infty}^{\infty} \frac{d\omega}{2\pi} [-\hat{\Sigma}_{\text{env}}^{\text{R}} \otimes \hat{G}^< + \hat{G}^< \otimes \hat{\Sigma}_{\text{env}}^{\text{A}} - \hat{\Sigma}_{\text{env}}^< \otimes \hat{G}^{\text{A}} + \hat{G}^{\text{R}} \otimes \hat{\Sigma}_{\text{env}}^<](\mathbf{k}, \omega; \mathbf{r}, t) \\ &= -\frac{1}{\hbar} \begin{pmatrix} 2\gamma_e[n_{\mathbf{k},e}(\mathbf{r}, t) - n_{\mathbf{k},e}^{\text{env}}(\mathbf{r}, t)] & 2\gamma[p_{\mathbf{k}}(\mathbf{r}, t) - p_{\mathbf{k}}^{\text{env}}(\mathbf{r}, t)] \\ 2\gamma[p_{\mathbf{k}}^*(\mathbf{r}, t) - p_{\mathbf{k}}^{\text{env}*}(\mathbf{r}, t)] & -2\gamma_h[n_{\mathbf{k},h}(\mathbf{r}, t) - n_{\mathbf{k},h}^{\text{env}}(\mathbf{r}, t)] \end{pmatrix}, \end{aligned} \quad (\text{S43})$$

where $\gamma = (\gamma_e + \gamma_h)/2$ and

$$n_{\mathbf{k},e}^{\text{env}}(\mathbf{r}, t) = \frac{\hbar}{2\gamma_e} \int_{-\infty}^{\infty} \frac{d\omega}{2\pi} [-\hat{\Sigma}_{\text{env}}^< \otimes \hat{G}^{\text{A}} + \hat{G}^{\text{R}} \otimes \hat{\Sigma}_{\text{env}}^<]_{11}(\mathbf{k}, \omega; \mathbf{r}, t), \quad (\text{S44})$$

$$1 - n_{\mathbf{k},h}^{\text{env}}(\mathbf{r}, t) = \frac{\hbar}{2\gamma_h} \int_{-\infty}^{\infty} \frac{d\omega}{2\pi} [-\hat{\Sigma}_{\text{env}}^< \otimes \hat{G}^{\text{A}} + \hat{G}^{\text{R}} \otimes \hat{\Sigma}_{\text{env}}^<]_{22}(\mathbf{k}, \omega; \mathbf{r}, t), \quad (\text{S45})$$

$$p_{\mathbf{k}}^{\text{env}}(\mathbf{r}, t) = \frac{\hbar}{2\gamma} \int_{-\infty}^{\infty} \frac{d\omega}{2\pi} [-\hat{\Sigma}_{\text{env}}^< \otimes \hat{G}^{\text{A}} + \hat{G}^{\text{R}} \otimes \hat{\Sigma}_{\text{env}}^<]_{12}(\mathbf{k}, \omega; \mathbf{r}, t). \quad (\text{S46})$$

This gives

$$\partial_t p_{\mathbf{k}}(\mathbf{r}, t) = -\frac{i}{\hbar} \left(\varepsilon_{\mathbf{k},e} + \varepsilon_{\mathbf{k},h} - \frac{\hbar^2 \nabla^2}{4m_{\text{eh}}} - 2i\gamma \right) p_{\mathbf{k}}(\mathbf{r}, t) + I_{\mathbf{k}}^{\text{pol}}(\mathbf{r}, t), \quad (\text{S47})$$

$$\partial_t n_{\mathbf{k},\sigma=e,h}(\mathbf{r}, t) + \mathbf{v}_{\mathbf{k},\sigma=e,h} \cdot \nabla n_{\mathbf{k},\sigma=e,h}(\mathbf{r}, t) = -\frac{2\gamma_{\sigma}}{\hbar} n_{\mathbf{k},\sigma=e,h}(\mathbf{r}, t) + I_{\mathbf{k},\sigma=e,h}(\mathbf{r}, t), \quad (\text{S48})$$

where $\mathbf{v}_{\mathbf{k},\sigma} = \hbar \mathbf{k} / m_{\sigma}$, and

$$I_{\mathbf{k},e}(\mathbf{r}, t) = \frac{2\gamma_e}{\hbar} n_{\mathbf{k},e}^{\text{env}}(\mathbf{r}, t) + \int_{-\infty}^{\infty} \frac{d\omega}{2\pi} [-\hat{\Sigma}_{\text{int}}^{\text{R}} \otimes \hat{G}^< + \hat{G}^< \otimes \hat{\Sigma}_{\text{int}}^{\text{A}} - \hat{\Sigma}_{\text{int}}^< \otimes \hat{G}^{\text{A}} + \hat{G}^{\text{R}} \otimes \hat{\Sigma}_{\text{int}}^<]_{11}(\mathbf{k}, \omega; \mathbf{r}, t), \quad (\text{S49})$$

$$I_{\mathbf{k},h}(\mathbf{r}, t) = \frac{2\gamma_h}{\hbar} n_{\mathbf{k},h}^{\text{env}}(\mathbf{r}, t) - \int_{-\infty}^{\infty} \frac{d\omega}{2\pi} [-\hat{\Sigma}_{\text{int}}^{\text{R}} \otimes \hat{G}^< + \hat{G}^< \otimes \hat{\Sigma}_{\text{int}}^{\text{A}} - \hat{\Sigma}_{\text{int}}^< \otimes \hat{G}^{\text{A}} + \hat{G}^{\text{R}} \otimes \hat{\Sigma}_{\text{int}}^<]_{22}(\mathbf{k}, \omega; \mathbf{r}, t), \quad (\text{S50})$$

$$I_{\mathbf{k}}^{\text{pol}}(\mathbf{r}, t) = \frac{2\gamma}{\hbar} p_{\mathbf{k}}^{\text{env}}(\mathbf{r}, t) + \int_{-\infty}^{\infty} \frac{d\omega}{2\pi} [-\hat{\Sigma}_{\text{int}}^{\text{R}} \otimes \hat{G}^< + \hat{G}^< \otimes \hat{\Sigma}_{\text{int}}^{\text{A}} - \hat{\Sigma}_{\text{int}}^< \otimes \hat{G}^{\text{A}} + \hat{G}^{\text{R}} \otimes \hat{\Sigma}_{\text{int}}^<]_{12}(\mathbf{k}, \omega; \mathbf{r}, t). \quad (\text{S51})$$

Equation (S48) is the desired Boltzmann equation (3) for $n_{\mathbf{k},\sigma}(\mathbf{r}, t)$.

We finally note that, the term $I_{\mathbf{k}}^{\text{pol}}(\mathbf{r}, t)$ in Eq. (S47) should vanish in the normal phase, since $p_{\mathbf{k}}(\mathbf{r}, t) = \lambda_{\text{cav}}(\mathbf{r}, t) = 0$ in this phase. The condensed phase is characterized by the order parameter (See Refs. [1–4] and the later discussion within the Hartree-Fock-Bogoliubov approximation as an example.).

$$\Delta_{\mathbf{k}}(\mathbf{r}, t) = \sum_{\mathbf{k}'} V_{\mathbf{k}-\mathbf{k}'} p_{\mathbf{k}'}(\mathbf{r}, t) - g \lambda_{\text{cav}}(\mathbf{r}, t). \quad (\text{S52})$$

Since $\Delta_{\mathbf{k}}(\mathbf{r}, t) = 0$ in the normal phase, $I_{\mathbf{k}}^{\text{pol}}(\mathbf{r}, t)$ can be written in the form,

$$I_{\mathbf{k}}^{\text{pol}}(\mathbf{r}, t) = \frac{i}{\hbar} \sum_{\mathbf{k}'} L_{\mathbf{k},\mathbf{k}'}(\mathbf{r}, t) \Delta_{\mathbf{k}'}(\mathbf{r}, t), \quad (\text{S53})$$

which gives our final form of the Boltzmann equation for $p_{\mathbf{k}}(\mathbf{r}, t)$ [Eq. (2) in the main text].

The other piece of interest is the dynamics of the photon amplitude $\lambda_{\text{cav}}(\mathbf{r}, t) = \langle a(\mathbf{r}, t) \rangle$, given by Eq. (3) in the main text. The Heisenberg equation of the photon annihilation operator $a(\mathbf{r}, t)$ is given by,

$$\begin{aligned} i\hbar\partial_t a(\mathbf{r}, t) = [a(\mathbf{r}, t), H] &= \left(\hbar\omega_{\text{cav}} - \frac{\hbar^2\nabla^2}{2m_{\text{cav}}} \right) a(\mathbf{r}, t) + g \sum_{\mathbf{k}, \mathbf{q}} e^{i\mathbf{q}\cdot\mathbf{r}} c_{-\mathbf{k}+\mathbf{q}/2, \text{h}}(t) c_{\mathbf{k}+\mathbf{q}/2, \text{e}}(t) \\ &+ \sum_{\mathbf{q}, \mathbf{Q}, i} \Gamma_{\text{v}} \psi_{\mathbf{Q}}(t) e^{i\mathbf{q}\cdot(\mathbf{r}-\mathbf{r}_i)} e^{-i\mathbf{Q}\cdot\mathbf{R}_i}. \end{aligned} \quad (\text{S54})$$

Taking the statistical average of Eq. (S54), we get,

$$i\hbar\partial_t \lambda_{\text{cav}}(\mathbf{r}, t) = \left(\hbar\omega_{\text{cav}} - \frac{\hbar^2\nabla^2}{2m_{\text{cav}}} \right) \lambda_{\text{cav}}(\mathbf{r}, t) + g \sum_{\mathbf{k}} p_{\mathbf{k}}(\mathbf{r}, t) + \left\langle \sum_{\mathbf{q}, \mathbf{Q}, i} \Gamma_{\text{v}} \psi_{\mathbf{Q}}(t) e^{i\mathbf{q}\cdot(\mathbf{r}-\mathbf{r}_i)} e^{-i\mathbf{Q}\cdot\mathbf{R}_i} \right\rangle. \quad (\text{S55})$$

By applying the Wick's theorem, as diagrammatically described in Fig. S2, we obtain

$$\begin{aligned} \left\langle \sum_{\mathbf{q}, \mathbf{Q}, i} \Gamma_{\text{v}} \psi_{\mathbf{Q}}(t) e^{i\mathbf{q}\cdot(\mathbf{r}-\mathbf{r}_i)} e^{-i\mathbf{Q}\cdot\mathbf{R}_i} \right\rangle &= N_{\text{t}} |\Gamma_{\text{v}}|^2 \int_{-\infty}^{\infty} dt' \sum_{\mathbf{Q}} B_{\text{v}}^{\text{R}}(\mathbf{Q}, t - t') \sum_{\mathbf{q}} e^{i\mathbf{q}\cdot\mathbf{r}} \langle a_{\mathbf{q}}(t') \rangle \\ &= N_{\text{t}} |\Gamma_{\text{v}}|^2 \int_{-\infty}^{\infty} dt' \int_{-\infty}^{\infty} \frac{d\omega}{2\pi} e^{-i\omega t'} \sum_{\mathbf{Q}} \hat{B}_{\text{v}}^{\text{R}}(\mathbf{Q}, \omega) \sum_{\mathbf{q}} e^{i\mathbf{q}\cdot\mathbf{r}} \langle a_{\mathbf{q}}(t') \rangle = -i\kappa \int_{-\infty}^{\infty} dt' \int_{-\infty}^{\infty} \frac{d\omega}{2\pi} e^{-i\omega t'} \sum_{\mathbf{q}} e^{i\mathbf{q}\cdot\mathbf{r}} \langle a_{\mathbf{q}}(t') \rangle \\ &= -i\kappa \lambda_{\text{cav}}(\mathbf{r}, t), \end{aligned} \quad (\text{S56})$$

where $B_{\text{v}}^{\text{R}}(\mathbf{Q}, \omega) = [\hbar\omega - \varepsilon_{\mathbf{Q}}^{\text{v}} + i\delta]^{-1}$ is the vacuum photon Green's function. This yields the desired Heisenberg equation [Eq. (3) in the main text].

HARTREE-FOCK-BOGOLIUBOV APPROXIMATION

We show here that Eqs. (1)-(3) reduces to the conventional polariton (condensate) picture, by showing within the Hartree-Fock-Bogoliubov approximation (HFBA) [1-4] that the matrix \hat{A} is given by [Eq. (7) ($\kappa = 0, \gamma \rightarrow 0^+, n_{\mathbf{k}, \sigma} \ll 1$) in the main text],

$$\hat{A}_{\text{BEC}} = \begin{pmatrix} \hbar\omega_{\text{cav}} & g_{\text{R}} \\ g_{\text{R}}^* & \hbar\omega_{\text{X}} \end{pmatrix}, \quad (\text{S57})$$

in the dilute equilibrium limit. The interaction part of the self-energy $\hat{\Sigma}_{\text{int}}$ within this approximation is given by,

$$\hat{\Sigma}_{\text{HFB}}^{\text{R}}(\mathbf{k}, \omega; \mathbf{r}, t) = - \begin{pmatrix} 0 & \Delta_{\mathbf{k}}(\mathbf{r}, t) \\ \Delta_{\mathbf{k}}^*(\mathbf{r}, t) & 0 \end{pmatrix}, \quad (\text{S58})$$

$$\hat{\Sigma}_{\text{HFB}}^{\text{A}}(\mathbf{k}, \omega; \mathbf{r}, t) = - \begin{pmatrix} 0 & \Delta_{\mathbf{k}}(\mathbf{r}, t) \\ \Delta_{\mathbf{k}}^*(\mathbf{r}, t) & 0 \end{pmatrix}, \quad (\text{S59})$$

$$\hat{\Sigma}_{\text{HFB}}^{\text{K}}(\mathbf{k}, \omega; \mathbf{r}, t) = \hat{\Sigma}_{\text{HFB}}^{\text{L}}(\mathbf{k}, \omega; \mathbf{r}, t) = 0. \quad (\text{S60})$$

We refer to Refs. [1-4] for the derivation. This yields,

$$I_{\mathbf{k}, \text{e}}(\mathbf{r}, t) = \frac{2\gamma_{\text{e}}}{\hbar} n_{\mathbf{k}, \text{e}}^{\text{env}}(\mathbf{r}, t) - 2\text{Im}[\Delta_{\mathbf{k}} p_{\mathbf{k}}^*], \quad (\text{S61})$$

$$I_{\mathbf{k}, \text{h}}(\mathbf{r}, t) = \frac{2\gamma_{\text{h}}}{\hbar} n_{\mathbf{k}, \text{h}}^{\text{env}}(\mathbf{r}, t) - 2\text{Im}[\Delta_{\mathbf{k}} p_{\mathbf{k}}^*], \quad (\text{S62})$$

$$I_{\mathbf{k}}^{\text{pol}}(\mathbf{r}, t) = \frac{1}{\hbar} [2\gamma p_{\mathbf{k}}^{\text{env}}(\mathbf{r}, t) + i\Delta_{\mathbf{k}}(\mathbf{r}, t) N_{\mathbf{k}}(\mathbf{r}, t)], \quad (\text{S63})$$

where $N_{\mathbf{k}}(\mathbf{r}, t) = 1 - n_{\mathbf{k}, \text{e}}(\mathbf{r}, t) - n_{\mathbf{k}, \text{h}}(\mathbf{r}, t)$ is the population inversion.

In the dilute equilibrium limit ($\kappa = 0, \gamma \rightarrow 0^+, N_{\mathbf{k}} \simeq 1$) in the steady state, the term $I_{\mathbf{k}}^{\text{pol}}(\mathbf{r}, t)$ simplifies to,

$$\begin{aligned} I_{\mathbf{k}}^{\text{pol}}(\mathbf{r}, t) &= \frac{i}{\hbar} \Delta_{\mathbf{k}}(\mathbf{r}, t) \\ &= \frac{i}{\hbar} \left[\sum_{\mathbf{k}'} V_{\mathbf{k}-\mathbf{k}'} p_{\mathbf{k}'}^0 - g \lambda_{\text{cav}}^0 \right] e^{-iEt/\hbar}, \end{aligned} \quad (\text{S64})$$

which gives $L_{\mathbf{k}, \mathbf{k}'}^{\text{eq, dil}} = \delta_{\mathbf{k}, \mathbf{k}'}$. In this case, from Eq. (S47),

$$\left(\frac{\hbar^2 \mathbf{k}^2}{m_{\text{eh}}} + (E_{\text{g}} - E) \right) \lambda_{\text{eh}}^0 \phi_{\mathbf{k}} = \sum_{\mathbf{k}'} V_{\mathbf{k}-\mathbf{k}'} \phi_{\mathbf{k}'} \lambda_{\text{eh}}^0 - g \lambda_{\text{cav}}^0. \quad (\text{S65})$$

For simplicity, let us assume that

$$\sum_{\mathbf{k}'} V_{\mathbf{k}-\mathbf{k}'} \lambda_{\text{eh}}^0 \phi_{\mathbf{k}'} \gg g \lambda_{\text{cav}}^0. \quad (\text{S66})$$

This assumption implies $g_{\text{R}} \ll E_{\text{X}}^{\text{bind}}$ (where g_{R} and $E_{\text{X}}^{\text{bind}}$ are the Rabi splitting and the exciton binding energy, respectively), as shown soon later. In this situation, Eq. (S65) reduces to the Schrödinger equation of an exciton,

$$\frac{\hbar^2 \mathbf{k}^2}{m_{\text{eh}}} \phi_{\mathbf{k}}^{\text{X}} - \sum_{\mathbf{p}} V_{\mathbf{k}-\mathbf{k}'} \phi_{\mathbf{k}'}^{\text{X}} = -E_{\text{X}}^{\text{bind}} \phi_{\mathbf{k}}^{\text{X}}, \quad (\text{S67})$$

or

$$\int d\mathbf{r}' \left[\delta(\mathbf{r} - \mathbf{r}') \frac{-\hbar^2 \nabla'^2}{m_{\text{eh}}} - V(\mathbf{r} - \mathbf{r}') \right] \phi_X(\mathbf{r}') = -E_X^{\text{bind}} \phi_X(\mathbf{r}), \quad (\text{S68})$$

where $\phi_{\mathbf{k}} = \phi_{\mathbf{k}}^X$ is the exciton wave function. Here, note that

$$|E_g - E| - E_X^{\text{bind}} \ll E_X^{\text{bind}}, \quad (\text{S69})$$

needs to be satisfied for Eqs. (S65) and (S67) to be compatible under the assumption (S66).

As a result, the off-diagonal components in the matrix

$$\hat{A} = \begin{pmatrix} h_{\text{cav}} & g_0 \\ \tilde{g}_0^* & h_{\text{eh}} \end{pmatrix}, \quad (\text{S70})$$

reduces to the Rabi splitting g_R ,

$$g_0 \simeq \tilde{g}_0 \simeq g\phi_X(\mathbf{r} = 0) = g_R, \quad (\text{S71})$$

and

$$\begin{aligned} h_{\text{eh}}^{\text{eq,dil}} &\simeq \sum_{\mathbf{k}} \left[\left(\frac{\hbar^2 \mathbf{k}^2}{m_{\text{eh}}} + E_g \right) |\phi_{\mathbf{k}}^X|^2 - \sum_{\mathbf{k}'} V_{\mathbf{k}-\mathbf{k}'} \phi_{\mathbf{k}'}^X \phi_{\mathbf{k}}^{X*} \right] \\ &= \sum_{\mathbf{k}} \left[\frac{\hbar^2 \mathbf{k}^2}{m_{\text{eh}}} \phi_{\mathbf{k}}^X - \sum_{\mathbf{k}'} V_{\mathbf{k}-\mathbf{k}'} \phi_{\mathbf{k}'}^X \right] \phi_{\mathbf{k}}^{X*} + E_g \\ &= -E_X^{\text{bind}} \sum_{\mathbf{k}} |\phi_{\mathbf{k}}^X|^2 + E_g = E_g - E_X^{\text{bind}} = \hbar\omega_X, \end{aligned} \quad (\text{S72})$$

which yields the desired Eq. (7). Since $|E_g - E| - E_X^{\text{bind}} = |E_g - E_-| - E_X^{\text{bind}} \sim g_R$ unless the system is not in an extreme red detuning, from Eq. (S69), our assumption (S66) is satisfied at $g_R \ll E_X^{\text{bind}}$.

DRIVEN-DISSIPATIVE GROSS-PITAEVSKII EQUATION (8)

Let us turn to the polariton laser regime, where the nonequilibrium condensate is dilute enough such that the polariton picture still holds, and show that the matrix \hat{A} in this regime is given by [6] (Eq. (8) in the main text),

$$\hat{A}_{\text{GP}} = \begin{pmatrix} \hbar\omega_{\text{cav}} - i\kappa & g_R \\ g_R^* & \hbar\omega_X + U_X |\lambda_{\text{eh}}^0|^2 + iR_X \end{pmatrix}. \quad (\text{S73})$$

In this regime, $\Delta L_{\mathbf{k},\mathbf{k}'} \equiv L_{\mathbf{k},\mathbf{k}'} - L_{\mathbf{k},\mathbf{k}'}^{\text{eq,dil}}$ that characterizes the derivation from the dilute equilibrium is small ($|\Delta L_{\mathbf{k},\mathbf{k}'}| \ll 1$). In this case, under the assumption (S66), we may approximate $\phi_{\mathbf{k}}$ as $\phi_{\mathbf{k}} \simeq \phi_{\mathbf{k}}^X$ giving $g_0 \simeq g_R$ and

$$\begin{aligned} E\lambda_{\text{eh}}^0 &= \tilde{g}_0^* \lambda_{\text{cav}}^0 + h_{\text{eh}} \lambda_{\text{eh}}^0 \\ &\simeq g_R \lambda_{\text{cav}}^0 + \left(\hbar\omega_X - \sum_{\mathbf{k},\mathbf{k}',\mathbf{p}} V_{\mathbf{k}-\mathbf{p}} \phi_{\mathbf{k}}^* \phi_{\mathbf{p}} \Delta L_{\mathbf{k},\mathbf{k}'} \right) \lambda_{\text{eh}}^0 \\ &\equiv g_R \lambda_{\text{cav}}^0 + (\hbar\omega_X + \Delta U + iR_X) \lambda_{\text{eh}}^0. \end{aligned} \quad (\text{S74})$$

Here, ΔU and R_X physically describe the blue shift of the exciton spectrum and the exciton gain, respectively. Expanding ΔU in terms of $|\lambda_{\text{eh}}^0|^2$ and neglecting the blue shift from the non-coherent part,

$$\Delta U \simeq U_X |\lambda_{\text{eh}}^0|^2, \quad (\text{S75})$$

we obtain the desired matrix \hat{A}_{GP} of the driven-dissipative Gross-Pitaevskii equation (8).

PROOF OF THE EXISTENCE OF A PHASE BOUNDARY WITH AN END POINT

Here, we prove the result in the main text: Whenever an exceptional point (EP) $\Omega = \sqrt{\varphi^2 + 4\tilde{g}_0^* g_0} = 0$ of the matrix \hat{A} (where $\varphi = h_{\text{cav}} - h_{\text{eh}}$), is found, there exists a phase boundary in its vicinity that ends at that point. Here, we assume that the matrix \hat{A} is a smooth function of the input parameters.

The central quantity for the proof is

$$\Lambda = \Omega^2 = \varphi^2 + 4\tilde{g}_0^* g_0 \quad (\text{S76})$$

that is directly related to the eigenvalues,

$$E_{\pm} = \frac{1}{2} [h_{\text{cav}} + h_{\text{eh}} \pm \Omega]. \quad (\text{S77})$$

We divide Λ into regions I-IV in terms of the sign of the real and imaginary part of Λ [Fig. S3(a)].

We prove the above theorem by showing that the matrix \hat{A} satisfies the following three properties:

1. Only the “+(-)”-solution can arise in region II (III).
2. Sweeping Λ from region III to II across the dotted line in Fig. S3(a) ($\text{Re}\Lambda < 0$ and $\text{Im}\Lambda = 0$) changes the solution type from “-” to “+” without discontinuity in the emission energy E , resulting in a smooth crossover.
3. In contrast, when sweeping parameters in a route where Λ encircles the EP as III \rightarrow IV \rightarrow I \rightarrow II, there must exist a point where the solution type switches discontinuously, resulting in a phase transition.

From the assumption that \hat{A} is a smooth function of the input parameters, these properties result in a phase boundary that ends at the EP, proving the theorem.

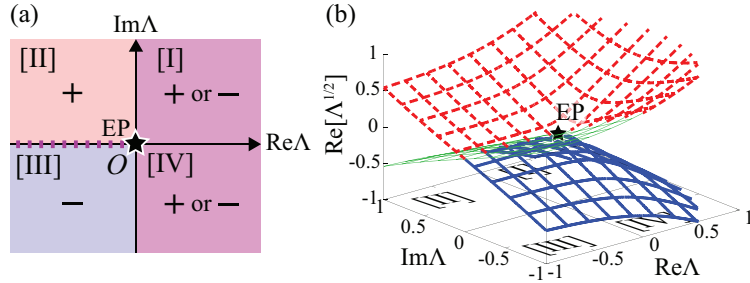


FIG. S3: (Color online) (a) Definition of regions I-IV. In region II (III), only “+(-)”-solution can be realized (property 1). (b) Plot of the real part of $\sqrt{\Lambda}$. The blue solid and the red dashed line represent different Riemann sheets, where the branch cut lies at $\text{Re}\Lambda < 0$ and $\text{Im}\Lambda = 0$ (the dotted line in panel (a)). The Riemann surface depicted in thin green lines is the sheet we do not use, due to the restriction from the property 1.

Let us first prove the property 1. The “-” and “+”-solutions satisfy

$$0 = E_- - E = \frac{1}{2} [2\xi - i(\kappa - R_{\text{eh}}) - \Omega], \quad (\text{S78})$$

$$0 = E_+ - E = \frac{1}{2} [2\xi - i(\kappa - R_{\text{eh}}) + \Omega], \quad (\text{S79})$$

respectively, where

$$\xi = \frac{1}{2} [\text{Re}[h_{\text{cav}}] + \text{Re}[h_{\text{eh}}]] - E, \quad (\text{S80})$$

$$R_{\text{eh}} = \text{Im}h_{\text{eh}}, \quad (\text{S81})$$

and

$$\Omega = \sqrt{\Lambda} = \sqrt{\tilde{\delta}^2 - (\kappa + R_{\text{eh}})^2 + 4\text{Re}[\tilde{g}_0^* g_0] - 2i[\tilde{\delta}(\kappa + R_{\text{eh}}) - 2\text{Im}[\tilde{g}_0^* g_0]]} \quad (\text{S82})$$

with $\tilde{\delta} = \text{Re}[h_{\text{cav}}] - \text{Re}[h_{\text{eh}}]$ and have taken $\text{Re}\Omega \geq 0$ among the two quantities that $\sqrt{\Lambda}$ takes. Note that, from the real part of Eqs. (S78) and (S79), the “-(+)-solution has $\xi \geq 0 (\leq 0)$ since we have defined $\text{Re}\Omega \geq 0$. Equations (S78) and (S79) both satisfy,

$$[4\xi^2 - (\kappa - R_{\text{eh}})^2] - 4i(\kappa - R_{\text{eh}})\xi = \Lambda, \quad (\text{S83})$$

or

$$\xi^2 = \frac{1}{4}[(\kappa - R_{\text{eh}})^2 + \text{Re}\Lambda] = \frac{1}{4}[-4\kappa R_{\text{eh}} + \tilde{\delta}^2 + 4\text{Re}[\tilde{g}_0^* g_0]], \quad (\text{S84})$$

$$4(\kappa - R_{\text{eh}})\xi = -\text{Im}\Lambda, \quad (\text{S85})$$

where we have used,

$$\text{Re}\Lambda = \tilde{\delta}^2 + 4\text{Re}[\tilde{g}_0^* g_0] - (\kappa + R_{\text{eh}})^2. \quad (\text{S86})$$

Equation (S85) gives,

$$\text{sgn}[\kappa - R_{\text{eh}}]\text{sgn}[\xi] = -\text{sgn}[\text{Im}\Lambda], \quad (\text{S87})$$

telling us that the sign of $\text{Im}\Lambda$ affects either the magnitude relation of κ and R_{eh} , or the solution type determined by the sign of ξ .

In fact, in regions II and III where $\text{Re}\Lambda < 0$, it can be shown that $\text{sgn}[\kappa - R_{\text{eh}}] = 1$ is always satisfied. From

Eq. (S84),

$$\begin{aligned} R_{\text{eh}} &= \frac{1}{4\kappa} [\tilde{\delta}^2 + 4\text{Re}[\tilde{g}_0^* g_0] - 4\xi^2] \\ &\leq \frac{1}{4\kappa} [\tilde{\delta}^2 + 4\text{Re}[\tilde{g}_0^* g_0]] \equiv R_{\text{eh}}^{\max}, \end{aligned} \quad (\text{S88})$$

where we have used $\kappa > 0$. In the region $\text{Re}\Lambda < 0$, from Eq. (S86), R_{eh}^{\max} satisfies,

$$R_{\text{eh}}^{\max} < \frac{1}{4\kappa}(\kappa + R_{\text{eh}})^2 \leq \frac{1}{4\kappa}(\kappa + R_{\text{eh}}^{\max})^2, \quad (\text{S89})$$

or

$$R_{\text{eh}} \leq R_{\text{eh}}^{\max} < \kappa. \quad (\text{S90})$$

As a result, from Eq. (S85), we get

$$\text{sgn}[\xi] = -\text{sgn}[\text{Im}\Lambda], \quad (\text{S91})$$

proving that only the “ $-$ (+)-solution given by $\xi > 0 (< 0)$ can be realized in region III (II).

We next show the properties 2 and 3. These properties can be understood from the plot of $\sqrt{\Lambda}$, depicted in Fig. S3(b). As seen in the figure, $\sqrt{\Lambda}$ is in general a multivalued quantity, consisting of multiple Riemann sheets (i.e., the sheets drawn with blue solid lines and red dashed lines). Noting our definition that $\text{Re}E_+ \geq \text{Re}E_-$, or $\text{Re}\Omega \geq 0$, it can be seen from Eq. (S77) that the Riemann sheet with $\text{Re}[\sqrt{\Lambda}] < 0 (> 0)$, depicted with blue solid lines (red dashed lines) in Fig. S3(b), is used in computing the emission energy E of the “ $-$ (+)-solution.

From the restriction of the solution types in regions II and III (property 1), we can ignore the Riemann sheet depicted with thin green lines in Fig. S3(b). Since the two Riemann sheets that are used for “ $-$ ” and “ $+$ ”-solutions

are connected at the boundary between regions II and III (i.e., the dotted line in Fig. S3(a)), the solution types can switch continuously by passing through that boundary, proving the property 2. Conversely, since that boundary is the only place that connects the two Riemann sheets, it is otherwise associated with exhibiting a discontinuity in physical quantities. This proves the property 3, and therefore the theorem.

* Electronic address: hanai@acty.phys.sci.osaka-u.ac.jp

- [1] R. Hanai, P. B. Littlewood, and Y. Ohashi, Phys. Rev. B **97**, 245302 (2018).
- [2] M. Yamaguchi, K. Kamide, T. Ogawa, and Y. Yamamoto, New J. Phys. **14**, 065001 (2012).
- [3] M. Yamaguchi, K. Kamide, R. Nii, T. Ogawa, and Y. Yamamoto, Phys. Rev. Lett. **111**, 026404 (2013).
- [4] M. Yamaguchi, R. Nii, K. Kamide, T. Ogawa, and Y. Yamamoto, Phys. Rev. B **91**, 115129 (2015).
- [5] J. Rammer, *Quantum Field Theory of Non-equilibrium States*, (Cambridge University Press, Cambridge, 2007).
- [6] M. Wouters and I. Carusotto, Phys. Rev. Lett. **99**, 140402 (2007).